BRIGHT WHITE LIGHT EMISSION OF ULTRASMALL NANOCRYSTALS FOR USE IN SOLID STATE LIGHTING

By

Sarah-Ann Michelle Harrell

Thesis

Submitted to the Faculty of the

Graduate School of Vanderbilt University

in partial fulfillment of the requirements

for the degree of

MASTER OF SCIENCE

in

Interdisciplinary Materials Science

May, 2013

Nashville, Tennessee

Approved:

Professor Sandra J. Rosenthal

Professor Sharon M. Weiss

ACKNOWLEDGEMENTS

First, I must acknowledge my advisor, Dr. Sandra Rosenthal. None of this would have been possible without you. Thank you for caring about your graduate students and for being so passionate and certain of the ideas that we work toward. The students in your lab turn into independent, strong scientists under your direction.

Second, I must thank Dr. Sharon Weiss for treating me as one of her own graduate students regardless of the lesser title, 'coadvisor.' You have this amazing way of gaining the respect of your graduate students while still keeping them on their toes.

I also want to thank the rest of my committee, Dr. Richard Haglund and Dr. Janet Macdonald. Dr. Macdonald, I will never forget your energy (even with a baby on the way) or your never-ending questions. I know you will be a great advisor to your future students. Dr. Haglund, I will never forget your knowledge of the world inside and outside of science or your ability to spark the curiosity of your students.

I must thank the Rosenthal group, and I wish the best of luck to every one of you. All of you have offered support at some point, some science related and some not. Thank you, Ian, for your willingness to always help. Thank you, Noah, for being such a great support and a down-to-earth person to talk to. Thank you, Joe, for the coffee talks and for advice on how to survive the first round of holidays as a married person. Thank you, James, for all the help with writing and ideas. Thank you, Emily,

for the many coffee dates and for all the valuable advice and support. Thank you, Oleg, for being so energetic when I felt so tired and for being a good listener.

In particular, I want to thank Toshia and Amy from the Rosenthal group. I can't imagine graduate school without you two. Thank you, Amy, for being patient with me when I felt like I just had to vent to someone; graduate school would have been much more difficult without your patience, help, support, and advice. Also, thank you for your giving spirit; I still feel like I owe you more than my bank account will allow from all the gifts you're constantly giving. Thank you, Toshia, for caring so much about not only me, but also about all the people around you, and for always having the desire to help people when you see a need. I'm always amazed at the lengths you go to when someone has a problem that needs fixing.

There are others at Vanderbilt that I would like to acknowledge and thank. Thank you, Robin Midgett, for the help with the Materials labs and for all of the South Street lunch dates. Thank you, Bobby Harl, for help with the RBS. I need to say thank you to the head and coordinator of my program, Dr. Greg Walker and Sarah Satterwhite. Both of you are wonderfully resourceful and helpful.

Next, it is essential to acknowledge my family. Without the financial and emotional support of my parents, my education would not have been possible. To my mom, thanks for your strong, compassionate, and disciplined example as a successful businesswoman. To my dad, your work-ethic, kindness, and interest in learning about the world around you outside of work has always inspired me. Also, thank you to both of you for allowing me to 'borrow' things and raid your fridge when the graduate student salary just wasn't enough. To my brother, Matt, I hope I

am as passionate about science as you are about history and politics, and I thank you for your never-ending love and support. To my husband, Jamey, thank you for being so incredibly understanding about the long hours I have spent in the lab and at home and for being so supportive in all of my career endeavors.

Last but certainly not least, I want to thank God for the opportunity to learn about His creation. Firstly, I am thankful to live in a place and time that is allowing me to follow my passion, and secondly, I am thankful to live in a world that is so interesting to learn about. My hope and wish is that I can somehow make this brilliant creation a better place.

This work was supported through Vanderbilt University and the National Science Foundation.

TABLE OF CONTENTS

Page

LIST OF TABLES

LIST OF FIGURES

LIST OF EQUATIONS

CHAPTER I

INTRODUCTION

1.1 The Problem with Lighting Today

In 1860, Joseph Swan invented the incandescent light that is still used today.[1] This light bulb works by converting electrical energy into heat through joule heating simultaneously producing light. Because most of the power put into an incandescent light bulb is converted to heat, incandescent light bulbs are among the most inefficient electrical equipment used in households today. The efficiency of lighting sources is often referred to as luminous efficacy and is typically measured in lumens/Watt (see Appendix A). The incandescent light bulb has a luminous efficacy of approximately 15 lumens/Watt (lm/W); however, a perfectly efficient white light source would have a luminous efficacy of over 200 lm/W.[2] When only taking into consideration the power that is put into the light bulb and the power that is successfully converted into white light, incandescent light bulbs have an efficiency of 5%.[1] Other household appliances display much better efficiencies including ovens, clothes dryers, and toasters at 70% and electric motors for fans at 90%.

According to a detailed study by the International Energy Agency in 2006 of the types and amount of lighting used around the world, the incandescent light bulb was still the preferred lamp in American homes at 91%.[3] In this study, the average lamp luminous efficacy was found to be 18 lm/W in the United States household, a stark contrast to other countries including Japan with an average lamp luminous

efficacy of 49 lm/W and Germany at 32 lm/W. [2, 3] The reason for the difference in efficacies is because other countries have been more rapidly converting to more efficient lighting, particularly compact fluorescent lamps (CFLs) which have luminous efficacies of around 50 lm/W. Partially due to the choice of using inefficient lighting, in 2005 North Americans used over twice as many watt-hours as Europeans did and over 4 times as many as the Japanese and Koreans combined.[3] The United States was the first to start a government-funded program to phase out incandescent lighting in 2007 and has decreased the amount of incandescent lumen-hours to 61% according to a 2012 study by the U.S. Department of Energy in 2012.[4,5]

The reasons often cited for the use of the incandescent light bulb include a lack of satisfaction with available lighting alternatives. More efficient lighting tends to have a greater upfront cost, a lack of dimmability, a cold and harsh color output, a different form factor compared to light bulbs originally designed for most lighting fixtures, and a limited amount of decorative arrangements.[3] While many of these issues have now been addressed for CFLs, another major concern with implementing CFLs into the home is the presence of about 5 mg of mercury in each CFL.[1] As of now, there are no special disposal method requirements or recommendations for CFLs in the United States due to the small number of light bulbs in use. Environmental concerns will become significantly more imperative as an increasing number of the incandescent lamps are replaced with CFLs.

Many of the aforementioned problems could be alleviated by converting to solid state lighting (SSL).[4] SSL is based on a simple concept in which electrons and holes are injected into and recombine in the junction region of a p-n semiconductor

device leading to the emission of light. SSL devices are known as light-emitting diodes (LEDs). The Department of Energy has predicted a slow switch over to SSL. Through the conversion of household lighting to LEDs, it is estimated that the equivalent of 2,700 terawatt-hours of electricity, representing at least $250 billion and 1,800 million metric tons of carbon, could be saved in the period from 2010 to 2030.[4]

One challenge inhibiting the successful conversion of household lighting to SSL is the color quality of commercially available white LEDs.[6] In order to produce high quality white light, a light source must emit light across the entire visible spectrum. However, semiconductors emit over a very narrow wavelength region. In the 1930s, the International Commission on Illumination (CIE) developed a quantitative way to measure the color of light called CIE coordinates with perfect white light being defined as $(0.33, 0.33)$ (see Appendix B).[2] However, having CIE coordinates of $(0.33, 0.33)$ is not the only important factor determining color quality. Incandescent lamps have a particularly high color rendering index (CRI) which means that the human eye perceives the color of an object to be the same when illuminated by daylight and the incadescent light source (see Appendix C).[1] Incandescent lamps also emit warm white light meaning that the white light has a yellow hue as opposed to a blue tint which is referred to as cool white light. The public prefers warm white light because cool white light is perceived as harsh. In the case of LEDs, white light is normally achieved by the combination of several different colors of LEDs or a combination of an LED with one or more phosphors. Figure 1.2 shows the three most common architectures for producing white LEDs.[7]

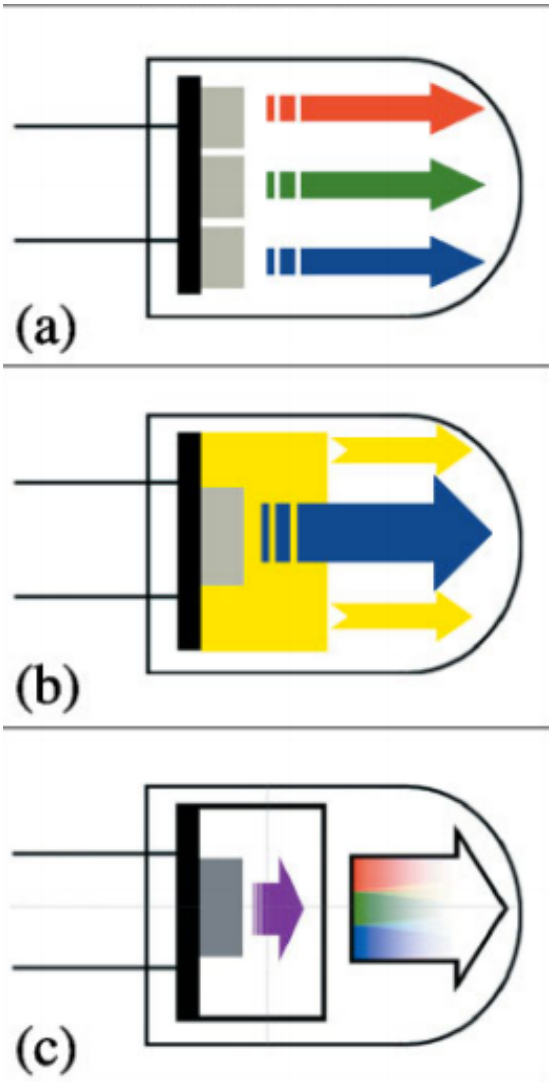

Figure 1.1. The three most common architectures to achieve white light are a.) an RGB LED, a mixture of red, green, and blue LEDs to make white light b.) a blue LED coated with a yellow phosphor, and c.) a near UV LED with a layer of red, green, and blue phosphors to create white light.[7]

The art of mixing monochromatic LEDs to obtain white light is often known as color mixing and can get very complicated as different color LEDs have different efficiencies and lifetimes. Mixing phosphors can lead to similar challenges, and the use of a monochromatic LED and single phosphor cannot produce a broad white

light spectrum. The Department of Energy Manufacturing Roadmap for SSL predicts that the production of consistent, good quality white light LEDs will be one of the major contributing factors to their increased cost compared to incandescent lamps and CFLs.[6]

1.2 Quantum Dots

When the diameter of a semiconductor is smaller than its Bohr exciton radius, electron-hole pairs created within the semiconductor are forced to orbit at a smaller radius than is energetically favorable; this confinement of the electron-hole pair enhances the band gap.[8] Consequently for semiconductors of this size regime, the band gap becomes dependent not only on the semiconductor material but also on the size of the semiconductor. These materials displaying a tunable band gap with size and, consequently, a tunable emission wavelength are called quantum dots. Quantum dots are typically under the classification of nanocrystals because, in order to reach the unique properties characteristic of quantum dots, the diameters of semiconductors must be on the order of a few nanometers. Some unique properties of quantum dots include very high absorption coefficients, high quantum yields, and surface chemistry flexibility which leads to a range of applications including fluorescent imaging, photovoltaics, and light-emitting diodes.[9-20]

Much research has been done on CdSe quantum dots due to their ability to emit over the entire visible spectrum through a variation in size. Figure 1.1 is a sampling of different sizes of CdSe nanocrystals ranging from a size of about 2 nm emitting blue light to a size of about 4 nm emitting red light.[8] Murray *et al.* was the

first to discover a reliable method of synthesizing CdSe nanocrystals that used a chemical, bottom-up approach in 1993.[21] This approach involved dimethyl cadmium as a Cd precursor, tri-n-octyl phosphine oxide (TOPO) as a coordinating solvent, and TOPSe as a Se precursor. Landes *et al.* was able to achieve CdSe nanocrystals at about 2 nm in size with this approach.[22] However, the reaction kinetics were too fast to be able to reach any sizes below 2 nm.

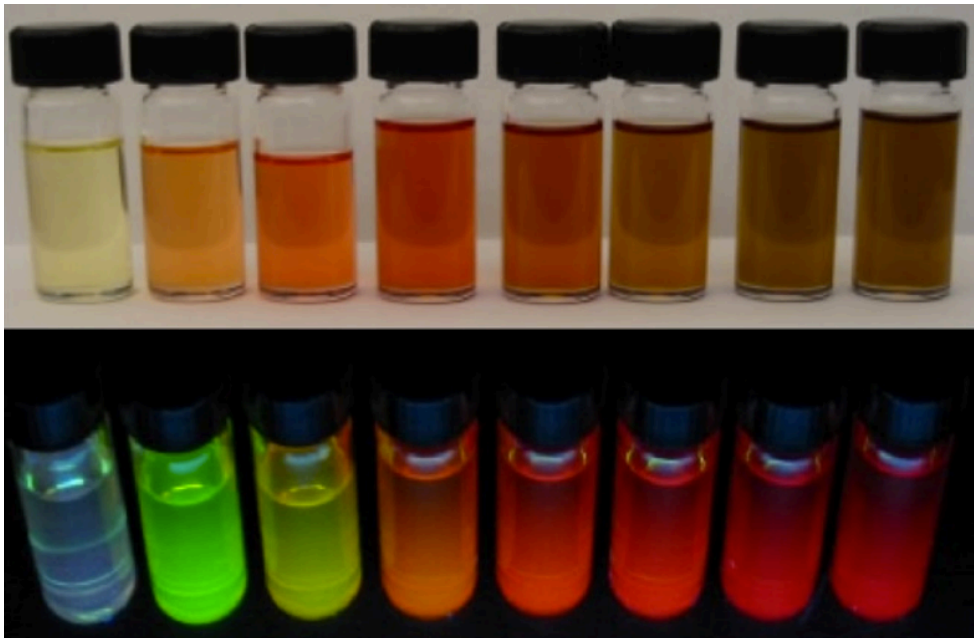

Figure 1.2. Vials of CdSe nanocrystals with increasing nanocrystal diameters from approximately 2 nm (left) up to approximately 4 nm (right). The vials are shown under room light in the top picture and are shown under UV light in the bottom picture.

In 2001, Peng *et al.* discovered CdO as a Cd precursor for CdSe nanocrystals which displayed much slower reaction kinetics; this allowed for the synthesis of sub-2 nm CdSe nanocrystals. Then, it was discovered that Cd-fatty acid complexes could also be used as Cd precursors and that they display the same slow kinetics.[22, 23] During the exploration of sub-2 nm nanocrystals, a subclass of CdSe nanocrystals

came about called magic-sized nanocrystals. Several groups reported the synthesis of CdSe magic-sized nanocrystals. Many of them were synthesized with fatty acid ligands while others were synthesized with phosphonic and phosphinic acids.[23-32] Magic-sized nanocrystals are nanocrystals that display a particularly stable configuration that results in little or no size distribution. Most nanocrystals under 2 nm in diameter are considered magic-sized nanocrystals.

1.3 Ultrasmall Nanocrystals

Bowers *et al.* desired to make sub-2 nm nanocrystals with phosphonic acid ligands.[33] With the phosphonic acid synthesis, an injection of Se:tributyl phosphine (Se:TBP) results in a nanocrystal nucleation at approximately 300°C. However, the growth of the nanocrystals at this temperature is too fast to expect sub-2 nm nanocrystals once the solution cools down. A method needed to be developed that would cool the reaction flask immediately after nucleation without affecting the reaction. The solution to the problem was a 'kill shot' in which 20 mL of butanol is injected immediately after the Se:TBP injection which cools the flask to 125°C. Then, the flask is further cooled to 90°C, the temperature at which growth stops.

As expected from their small size, Bowers' nanocrystals exhibited a near-UV band gap around 414 nm. One would expect these nanocrystals to have not only band gap emission, but also 'deep-trap' emission since most nanocrystals below 3 nm possess this surface-related trap state.[28-30, 32, 34-37] However, the observed emission spectrum consisted of three broad peaks spanning the visible region including a blue peak, green peak, and the red 'deep-trap' emission peak. Together,

these three peaks combine to produce all of the colors needed to make white light. An example absorption and emission spectrum of CdSe nanocrystals synthesized by Bowers' method is shown in Figure 1.3. Remarkably, the CIE coordinates indicate almost perfect white light at (0.31, 0.33). For the first time, a semiconductor was shown to emit almost perfect white light similar to the color quality of noontime sunlight.

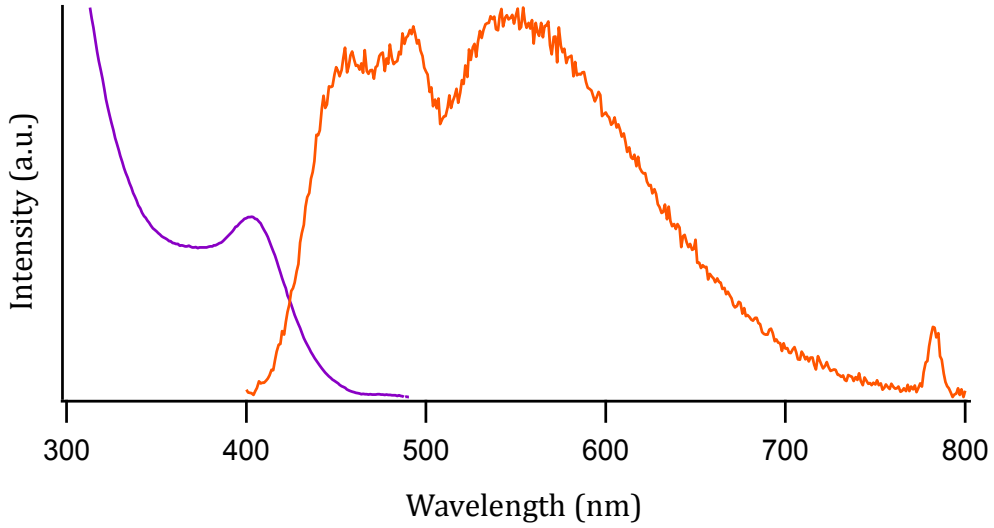

Figure 1.3. An example absorption (purple) and emission (orange) spectrum of ultrasmall CdSe nanocrystals. The emission spectrum displays three distinct peaks centered at approximately 450, 490, and 550 nm known as the blue, green, and red 'deep-trap' peak, respectively.

The aforementioned sub-2 nm CdSe nanocrystals were thought to be magic-sized nanocrystals.[33] Later, it was clear that these nanocrystals were not magic-sized but, instead, displayed the same growth properties as the larger, more traditional nanocrystals. As with larger nanocrystals, the size distribution of these

sub-2 nm CdSe nanocrystals is dependent on the synthesis, particularly the rapidity of the Se:TBP injection, indicating that there is not just one especially stable configuration as is the case with magic-sized nanocrystals. Therefore, not only are these nanocrystals the only semiconductors that can emit almost perfect white light, they are also among the few quantum dots of sub-2 nm size that are not magic-sized.[22, 33, 38] The sub-2 nm CdSe nanocrystals first reported by Bowers *et al.* are a new subclass of quantum dots called ultrasmall nanocrystals.[33]

The presence of the blue and green emission peaks in addition to the well-known, broad deep-trap emission in the red is a characteristic property of the ultrasmall CdSe nanocrystals. The blue peak corresponds the emission peak at 445 nm, and the green peak corresponds to the emission peak at 488 nm as shown in Figure 1.3.[39, 40] The blue and green peaks appear very abruptly in the emission spectrum when the nanocrystals are synthesized with an absorption band gap smaller than 420 nm.

Schreuder *et al.* showed that the blue peak is directly associated with the ligand bound to the Cd at the surface of the nanocrystal.[39] The exact wavelength as well as the ratio of the intensity of this peak in comparison to the intensity of the other peaks in the ultrasmall nanocrystals can be modified by using different phosphonic acids as ligands. The wavelength of the blue peak is correlated to the electronegativity of the ligand, and the intensity of the blue peak is correlated to the length of the carbon chain. It is very clear that this highest energy emission peak is not the band gap emission for three reasons. First, the Stokes shift is 25 to 45 nm depending on the exact size of nanocrystals synthesized which is too large to be due

to the band gap. Second, the wavelength of this peak does not change with the nanocrystal size as Schreuder *et al.* showed but instead with the choice of surface ligand used. Interestingly, while the blue peak wavelength does not change with nanocrystal size, the absorption peak of the ultrasmall CdSe nanocrystals does change with size as expected from the quantum confinement effect. Dukes *et al.* referred to these first two reasons as pinned emission; the absorption continues to change with size, but the emission is remains unchanged.[41] Third and most importantly, ultrafast spectroscopy revealed that the decay kinetics of each of the white light emission features are similar to those measured for trap state emission, rather than true bandgap emission.[40]

A way to systematically modify the green peak has not yet been found; changing the surface ligands does not appear to have an effect on this peak. From the myriad of nanocrystals that have been synthesized in this size regime with carboxylic acids, it is clear that the surface state causing the green peak does not exist for fatty acid-capped nanocrystals.[22, 30, 31, 42-44] Therefore, this extra surface state may relate to the phosphonic/phosphinic acid functional group. The green peak was also present in the weak emission spectrum of the magic-sized nanocrystals made by Dukes *et al.* with diisoocytlphosphinic acid.[34] There are other sub-2 nm nanocrystals made with phosphonic acid ligands including Peng *et al.* which did not provide information on the nanocrystals' emission. Owen *et al.*'s nanocrystal emission spectrum taken 30 s after nucleation did seem to have a slight shoulder in the 490 nm region.[24, 45] Cossairt *et al.* reported magic-sized nanocrystals with emission affected by the ligands.[35] However, the emission was

phosphorescence from the ligands themselves rather than a surface trap on the nanocrystal. The ligands of the ultrasmall CdSe nanocrystals do not emit by themselves, so the blue and green peaks must be due to emission from the nanocrystal with strong evidence supporting that the emission is surface-related.

1.4 Quantum Dot White LEDs

Quantum dots (QDs) have been used extensively to make white LEDs.[46-51] Their high quantum yields and ease of mixing render them particularly advantageous for making bright white LEDs. Table 1.1 shows color characteristics of some quantum dot LEDs.[46, 52-59] Most QD LED structures involve the mixing of different color QDs together into one film. This can get complicated and time-consuming. One can try estimating how much of each color must be incorporated into a film in order to make good quality white light by simulations.[46] However, this would have to be done after the syntheses of all of the colors due to insufficient size control over QDs.

Table 1.1. Color characteristics and structure for some quantum dot white LEDs.

Type	Structure	CIE Coordinates	CRI	Reference
Electroluminescent	Mixed QDs	(0.35, 0.41)	86	Ziegler *et al.*[52]
Phosphor-based	Mixed phosphor and QD	(0.29, 0.30)	90	Jang *et al.*[53]
Electroluminescent	Layers of QD and emitting polymer	(0.32, 0.37)	NA	Demir *et al.*[46]
Phosphor-based	Mixed QDs	(0.30, 0.28)	71	Nizamoglu *et al.*[59]
Phosphor-based	Mixed QDs	(0.33, 0.33)	91	Chen *et al.*[55]
Phosphor-based	QD-QW particles	(0.36, 0.30)	75	Nizamoglu *et al.*[56]
Phosphor-based	Close-packed QD films	(0.44, 0.40)	NA	Nizamoglu *et al.*[58]
Phosphor-based	1 type of QD: ultrasmall CdSe	(0.33, 0.33)	97	Schreuder *et al.*[57]

Ultrasmall nanocrystals may be ideal candidates for applications in white LEDs.[29, 38, 57, 60] Schreuder *et al.* was able to incorporate these nanocrystals into photoluminescent and electroluminescent solid-state devices.[57, 60] The photoluminescent devices consisted of ultrasmall nanocrystals encapsulated in a polymer, biphenyl-perfluorocyclobutyl (BP-PFCB), that coated a UV LED as shown in the inset in Figure 1.4.[60] The BP-PFCB polymer was chosen because it did not have an effect on the white light spectrum of the nanocrystals. As can be seen in the graph of Figure 1.4, there is very little difference between the spectrum of the nanocrystals in solution and the spectrum of the nanocrystals in the polymer. An efficiency of about 1 lm/W was achieved utilizing these devices.[60]

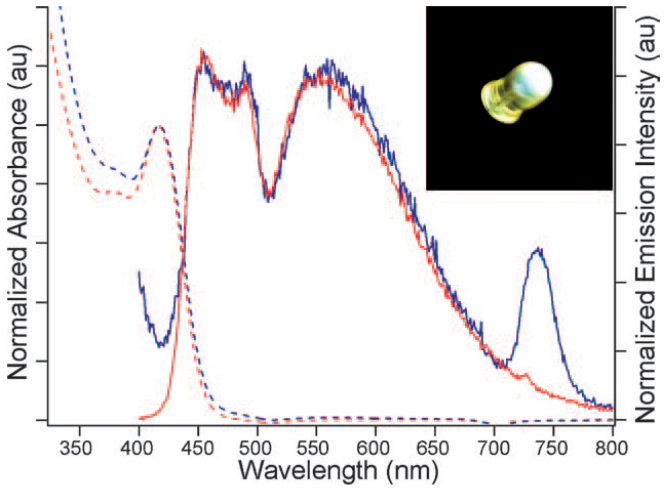

Figure 1.4. Absorption and emission of CdSe white light nanocrystals. The dashed lines show the absorption spectrum, and the continuous lines show the emission spectrum of nanocrystals encapsulated in the BP-PFCB polymer (blue), BP-PFCB, and nanocrystals in solution (red). Inset: encapsulated nanocrystals coating a UV LED to make a white LED.

The blue and green peaks combined with deep trap emission in the red wavelengths of the ultrasmall nanocrystal emission spectrum creates almost perfect white light.[61] However, a major drawback of using these nanocrystals in LED applications is their low quantum yield of around 10%. Quantum yields of nanocrystals have been reported as high as 85%, so a method of increasing the quantum yield must be found in order for the use of ultrasmall nanocrystals in white LEDs to be viable.[62]

Since ultrasmall nanocrystals emit via surface-related states, conventional brightening methods cannot be used. A standard and demonstrated method of brightening nanocrystals is called shelling and is done by synthesizing an inorganic shell of a wider band gap material to surround the nanocrystal; this confines the electron-hole pair to the core nanocrystal.[63, 64] Unfortunately, this method does not enhance the three peaks that produce white light for ultrasmall nanocrystals.

Instead, the inorganic shell modifies the surface of ultrasmall CdSe nanocrystals to emit via the band gap resulting in the emission of a sharp peak with a much smaller Stokes shift in the ultraviolet/blue region.[40, 65] In order to retain the purity of the white light emission, any additional passivation of ultrasmall CdSe nanocrystals must enhance the original three emission peaks equally. These emission peaks are caused by the phosphonic acid passivation layer, so this passivation layer cannot be replaced by ligand exchange or an inorganic shell.

Rosson *et al.* found that by mixing the nanocrystals with formic acid while heating the solution, the three peaks in the white light spectrum could be enhanced to achieve a quantum yield as high as 45%.[61] The enhancement of these peaks as well as an inset picture comparing treated ultrasmall nanocrystals with original ultrasmall nanocrystals is shown in Figure 1.5. The treated nanocrystals are evidently brighter, but they are also more blue-white in color. It is still unclear whether the increase in quantum yield is caused by a ligand exchange or whether the formic acid is binding somewhere on the nanocrystal in addition to the dodecylphosphonic acid (DDPA). However, Rosson *et al.* claims that complete ligand exchange is unlikely because the blue and green peaks which seem to be related to the phosphonic acid ligand are still intact. From Figure 1.5 shows that the absorption peak is slightly blue shifted following the formic acid treatment, indicating that the formic acid may have etched a small amount of the surface of the nanocrystal.

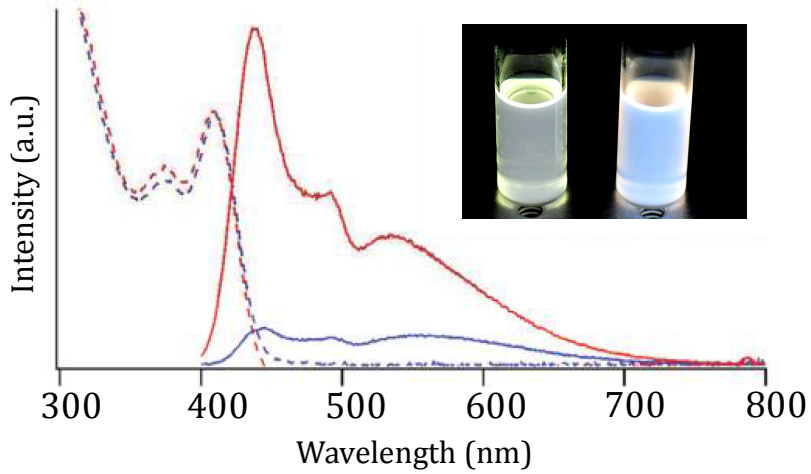

Figure 1.5. The dashed lines represent the absorption spectrum before the treatment (blue) and after the treatment (red). The solid lines show the emission spectrum of the nanocrystals before the treatment (red) and after the treatment (blue). Inset: vials containing a concentrated solution of untreated (left) and treated (right) nanocrystals.

1.5 Incorporating Ultrasmall CdSe Nanocrystals into an LED

By incorporating formic acid-treated ultrasmall nanocrystals with a quantum yield of 40% into an LED, one should be able to achieve a luminous efficacy of about 3.8 lm/W (See Appendix A). However, the method reported by Rosson *et al.* does not reproducibly lead to such an enhancement.[61] The average quantum yield achieved was 31% with a standard deviation of 6%. Further studies are needed to clarify the reason for the large standard deviation and to be able to consistently achieve high quantum yields. The molar excess of formic acid to nanocrystals, the concentration of the nanocrystal solution, the lighting environment of the treatment, the use of solvents in the treatment, the reaction time of the treatment, and parameters of the original ultrasmall synthesis before treatment are all ways in which the treatment could be altered to produce the desired results.

CHAPTER II

EXPERIMENTAL

2.1 Ultrasmall Nanocrystal Synthesis

The nanocrystals were prepared by slightly modified methods from Bowers *et al*.[33] For a typical ultrasmall nanocrystal synthesis, 0.2 M Se:TBP solutions were prepared in a glove box. 6 g tri-n-octylphosphine oxide (TOPO), 4 g hexadecylamine (HDA), 0.51 g dodecylphosphonic acid (DDPA, 2.0 mmol), and 0.128 g cadmium oxide (CdO, 1.0 mmol) were loaded into a three-neck round bottom 100 mL flask; one side neck was fitted with a temperature probe and the other with a rubber septum. The center neck was fitted with a self-washing bump trap through which argon gas was flowed. The mixture was stirred and heated to 150°C while being purged with a 12-gauge needle in the rubber septum. After removing the needle, the solution was allowed to continue heating to 330°C and was kept at 330°C until conversion of CdO to the Cd-phosphonate complex was complete when all of the brown CdO has reacted forming a clear, colorless solution. Then, 4.0 mL of Se:TBP (0.80 mol) solution is pulled directly through the Teflon cap of the bottle into a syringe fitted with a 6 in. 22-gauge needle and is rapidly injected into the flask using a 1.5 in. 12-gauge needle through the rubber septum. When the nucleation of nanocrystals was indicated by a change in color of the solution from colorless to a pale yellow, 20 mL of butanol was rapidly injected using an 18-gauge needle

lowering the temperature to about 125°C. The reaction was then immediately cooled to 90°C with compressed air.

The nanocrystals were cleaned using a three-step centrifugation method. The reaction solution was evenly divided between four 30 mL centrifuge tubes and was precipitated by methanol. The tubes were spun at 6000 rpm for 3 minutes producing a large, pale yellow, powdery pellet. The supernatant was decanted, and the pellet was suspended in 6 mL of hexanol for each tube. Often, a Fisher Scientific FS30D ultrasonicator was used briefly to aid in this suspension. This suspension was spun at 6000 rpm for 20 minutes producing a white pellet. The supernatant was poured into four other centrifuge tubes and was precipitated again with methanol. The tubes were spun at 6000 rpm for 20 minutes. A small gel-like yellow pellet was produced; the supernatant was decanted, and the pellet was dissolved in toluene. This solution was stored in the dark.

2.2 The Formic Acid Treatment

Rosson *et al.*'s formic acid treatment was employed to brighten the nanocrystals.[61] Treatments were done by injecting 5 mL of the solution of nanocrystals at a concentration of 0.3-1 mM into a 50 mL three neck flask with no direct light on the flask. The nanocrystals were heated and vigorously stirred. 30,000 molar excess of formic acid to nanocrystals was added to the flask once the solution reached a temperature of 24°C. The mixture was allowed to continue heating at about seven degrees per minute; once it reached 60°C, the mixture was immediately cooled with compressed air down to 28°C. Then, the solution was

transferred to a glass vial in which it was spun at 2500 rpm for 15 minutes. The top toluene layer containing nanocrystals was transferred to 2 mL centrifuge tubes and was spun at 15,500 rpm for 15 minutes. The resulting top layer was put into a vial and stored in the dark.

2.3 Assessments and Variations on the Formic Acid Treatment

In order to evaluate whether the formic acid treatment was a permanent or temporary enhancement, longevity experiments were performed on treated nanocrystals. The quantum yield of three different batches of treated nanocrystals was measured about every other day for 18 days after treatment.

The molar excess of formic acid to nanocrystals, the concentration of the nanocrystal solution, the lighting environment of the treatment, the use of solvents in the treatment, the reaction time of the treatment, and parameters of the original ultrasmall synthesis were all varied with the goal of achieving a consistently high quantum yield of near 40%. The molar excess of formic acid to nanocrystal was varied from about 15,000 to about 65,000 by changing the volume of formic acid added to the flask for each treatment. The concentration range of the nanocrystal solution was varied from $\sim 1.00\times10^{-3}$ to $\sim 2.06\times10^{-4}$ M. Based on a prior report that the lighting environment during the formic treatment of ultrasmall CdSe nanocrystals affected the resulting quantum yield, different lighting environments were tested including UV light shining on the flask with room and hood lights on, UV light shining on the flask with room and hood lights off, visible light on the flask

(room and hood lights on), and no visible light on the flask (room and hood lights off with Al foil over the reaction flask).[66]

In order to explore the effects of using different solvents other than toluene in the formic acid treatment, the ultrasmall nanocrystals were dissolved/suspended in the following solvents directly after synthesis: methanol, butanol, hexanol, isopropanol, mesitylene, trichloroethylene, chloroform, and hexanes. For the solvents that were less miscible with the nanocrystals including methanol, butanol, and isopropanol, the nanocrystals were suspended in the solvent directly after the synthesis of the nanocrystals using a sonicator. Then, a treatment was done on the nanocrystals immediately. In these cases, the nanocrystals formed a pellet after the first centrifugation step. This pellet was dissolved in toluene and taken to the fluorometer for a quantum yield measurement.

The reaction time was varied in two different ways prepared to the protocol initially developed for the treatment in which the reaction solution was heated from 24°C to 60°C in about 5 minutes time. In this work both a slower heating ramp-up of about 10 minutes which increased the reaction time and a faster heating ramp-up of about 3 minutes which reduced the reaction time was also explored. The reaction was also held after heating at about 60°C for extended periods ranging from about 5 minutes to 2 hours. Room temperature treatments following the previously reported protocol, but without heating were also carried out for durations ranging from 10 minutes to 3 hours.

During the course of this research, it was empirically found that the quality of the synthesized nanocrystals varied significantly from batch to batch with the Se

concentration in TBP appearing to directly influence the final quantum yield both before and after treatment. Accordingly, batches of nanocrystals were made in which the Se:TBP concentration was varied from 0.2 M to 0.7 M in 0.1 M increments. These nanocrystals were treated, and the quantum yields were measured before and after treatment.

2.4 Phosphor-based LEDs

Phosphor-based LEDs were made with treated and untreated nanocrystals using Schreuder *et al.*'s method with slight variations.[60] Modeled after glass vial bottoms that had been cut off, glass dishes with walls 1 cm high and diameters 2.75 cm long were made to hold the encapsulated nanocrystal films. These dishes were washed by placing them in a floating petri dish in a Fisher Scientific FS30D Sonicator and sonicating for 15 minutes with acetone and 15 minutes with isopropanol. Then, they were put into the oven to dry.

Depending on the number and thickness of films desired, 30 to 70 mg of biphenylperfluorocyclobutyl (BP-PFCB) polymer was placed into a small, clean glass vial. The polymer was dissolved in mesitylene in a 20 wt% ratio of polymer to solvent. Then, a very concentrated solution of nanocrystals in mesitylene was added to the glass vial in weight loadings of nanocrystals to polymer ranging from 2 to 10 wt%. This solution was vigorously stirred with a baby stir bar for about 30 minutes. Then, 0.5 to 1.25 mL of the nanocrystal/polymer solution was pipetted into each glass dish depending on the desired thickness of the film. The resulting thickness

was determined by the amount of polymer and nanocrystals put into each glass dish and had to be tweaked to get desired results.

The films were annealed under N_2 overnight at ~70°C on a hotplate in a hood. Figure 2.1 shows the set-up of the annealing apparatus. The glass dishes were placed directly into a sand-filled container, as shown in the figure. The N_2 was flowed into the set-up through a tube connected to an N_2 tank. This tube was fitted with a long pipet; the thin part of the pipet was put into the heating apparatus through a hole in the top. The temperature of the set-up was determined by putting a temperature probe through the top of the set-up before introducing N_2.

Figure 2.1. Annealing apparatus for the encapsulation of ultrasmall nanocrystals.

2.5 Characterization

After synthesis, a Varian Cary 50 Bio ultraviolet-visible (UV-Vis) spectrophotometer was used to characterize the absorption of the nanocrystals. The band gap wavelength, absorbance, and Peng *et al.*'s equations were used to find

the molar concentration and the size of the nanocrystals.[67] In order to do this, the diameter (D) is first found using Equation 2.1 where λ is the band gap absorption wavelength. Once the diameter is known, the extinction coefficient can be found using Equation 2.2 where ΔE is the band gap in eV.

$$D = (1.6122\times10^{-9})\lambda^4 - (2.6575\times10^{-6})\lambda^3 + (1.6242\times10^{-3})\lambda^2 - (0.4277)\lambda + (41.57) \quad (2.1)$$

$$\epsilon = 1600\Delta E(D)^3 \quad (2.2)$$

Quantum yield measurements were taken the same day of treatment by comparing the absorption and emission of the nanocrystal solution to Coumarin 152A at an excitation wavelength between 385 nm and 395 nm. The nanocrystal emission was measured using an ISS PC1 Photon Counting Spectrofluorometer. Equation 2.3 shows the calculation performed to determine the quantum yields.[68]

$$QY_{NC} = \left(\frac{E_{NC}/A_{NC}}{E_{STD}/A_{STD}}\right) \times \left(\frac{\eta_{NC}}{\eta_{STD}}\right)^2 \times QY_{STD} \quad (2.3)$$

E_{NC} and E_{STD} are the integrated emission intensities from 400 nm to 800 nm of the nanocrystals and the standard dye, respectively. A_{NC} and A_{STD} are the absorbance values of the nanocrystals and standard dye at the excitation

wavelength. η_{NC} and η_{STD} are the indices of refraction for the solvents of the nanocrystal solution and the standard dye solution, typically toluene and ethanol, respectively. QY_{NC} and QY_{STD} are the quantum yield of the nanocrystals and the standard dye; the quantum yield of the standard dye is 38%.

Preliminary Rutherford Backscattering (RBS) was also performed on untreated nanocrystals to determine the Se:Cd ratio. Samples were prepared on 1x1 cm graphene substrates that were cleaned with chloroform. A solution of nanocrystals dissolved in toluene with a concentration of $\sim 10^{-4}$ M was dropcasted on the substrates; after the substrates were dry, the dropcasting was repeated one more time. The samples were taken for analysis using the Pelletron source at Vanderbilt with a 2 MeV He^{2+} beam.

Measurements of the ultrasmall CdSe nanocrystal phosphor-based LEDs were perormed on an SLMS 400 Integrating Sphere from Labsphere with a CDS 500 Spectrometer. The encapsulated nanocrystals were placed on top of a Nichia 385 nm UV LED which was powered by a Keithley 2400 source meter. Devices displaying different weight loadings and thicknesses were measured using this setup to evaluate their luminous efficacy.

CHAPTER III

RESULTS AND DISCUSSION

3.1 Formic Acid Treatment Experiments and Modifications

The longevity of the formic acid treatment was measured and is depicted in Figure 3.1 for three typical batches of nanocrystals. The quantum yield increased by 10% after the first day and then slowly decreased in quantum yield over the course of 18 days. The quantum yield was actually higher than the quantum yield measured on the day of the treatment. These results suggest that the treatment is not temporary, although longer term studies have not been performed.

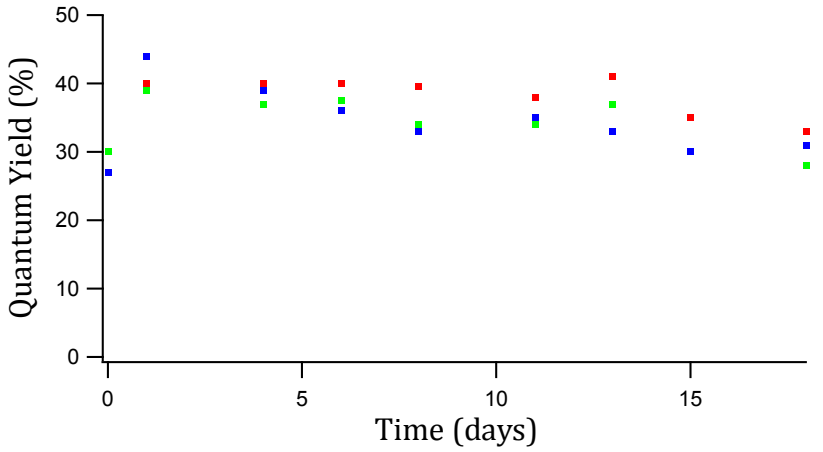

Figure 3.1. Quantum yield results of longevity experiments. Each color represents a particular batch of treated nanocrystals.

The molar excess of formic acid to nanocrystals used in the treatment was varied from 15,000 to 65,000. Table 3.1 gives the average quantum yield and standard deviation of the different molar excesses. A trend between the molar excess and the quantum yield could not be made. However, since the nanocrystals synthesized with the largest values of molar excess of formic acid tended to give higher quantum yields, a molar excess of 65,000 was selected for the remainder of the experiments described in this thesis. Note that there was no noticeable difference in the shape of the nanocrystals emission spectra when the molar excess of formic acid was varied further suggesting that the molar excess of formic acid is not the most important factor in the treatment.

Table 3.1. Formic acid to nanocrystal molar excess effects on quantum yield

Molar Excess	Average Quantum Yield (%)	Standard Deviation (%)	Number of Trials
20,000	27	NA	1
25,000	26	NA	1
30,000	25	6	4
35,000	20	NA	1
40,000	22	NA	1
45,000	32	NA	1
50,000	22	NA	1
55,000	29	4	3
60,000	28	NA	2
65,000	34	6	3

Limited experiments were performed to investigate the influence of the concentration of the nanocrystal solution in the reaction flask during formic acid treatment. With two different batches of nanocrystals and with concentrations

ranging from 1.00×10^{-3} to 2.06×10^{-4} M, the resulting quantum yield was relatively constant near 20%. Again, no trend could be concluded from the results.

When the reaction flask was placed under variable lighting environments, there was a noticeable drop in the quantum yield when UV light was illuminated on the flask. However, no noticeable effect on the quantum yield was measured when the reaction was performed with or without visible light. Remaining experiments were performed under visible light.

Formic acid and toluene have low miscibility; hence, vigorous stirring is essential for the treatment to be effective. Experiments were performed using the same treatment method described by Rosson *et al.* but in different solvents to investigate whether improved miscibility between formic acid and the solvent in which the nanocrystals were suspended would make the treatment more effective.[61] After synthesis, the ultrasmall CdSe nanocrystals were suspended in a variety of solvents including chloroform, methanol, butanol, isopropanol, mesitylene, trichloroethylene, and hexanol. The treatment was then carried out with no other modifications with these different solvents. The use of cosolvents was also attempted in 1:6 ratios of isopropanol and butanol to toluene. It must be noted that for some of the solvents that were tested, the nanocrystals became completely insoluble in all tested solvents after the treatment so that they could not be dissolved for a quantum yield measurement. It is possible that in these cases the nanocrystals might have been stripped of their ligands; the etching of the nanocrystal by the formic acid might have been more favorable in the environment of these solvents. When isopropanol was used as the sole solvent, the results were

inconsistent, and the nanocrystals often became (this occurred for four out of six trials). Table 3.2 displays the quantum yields that were obtained after treatments with the solvents that did not cause the nanocrystals to become insoluble.

Table 3.2. Quantum yield results after the formic acid treatment with different solvents.

Solvent	**Quantum Yields (%)**
methanol	12
isopropanol	17/12
butanol	11
2:3 of isopropanol to toluene	10
1:6 of isopropanol to toluene	10
1:6 of butanol to toluene	12
trichloroethylene	17
chloroform	17
hexanes	16/15

Good miscibility with both the nanocrystals and the formic acid was achieved with chloroform, trichloroethylene, and with the use of cosolvents. However, in all of these cases, the treatment had little effect on the nanocrystal emission as can be seen in Table 3.2. The only other solvent that could reproduce a similar quantum yield enhancement after treatment compared to toluene was mesitylene which gave an average quantum yield of 29% for 9 trials. A possible explanation for this phenomenon is that the formic acid is drawn to the nanocrystal surface only when it prefers this environment over the environment of the solvent. Therefore, it only works when the miscibility between the solvent of the nanocrystals and the formic acid is sufficiently low.

An example spectrum of nanocrystal emission after a formic acid treatment with hexanes as the nanocrystal solvent is shown in Figure 3.2. Although the quantum yield was not as high compared with a treatment performed using toluene, the use of hexanes did yield a relatively consistent quantum yield of around 15% with improved CIE coordinates. The difference in peak enhancement might suggest that there is more than one binding site for formic acid. It seems that in all cases, the combination of using mesitylene/toluene as a solvent and formic acid as the carboxylic acid in the treatment causes a further enhancement of the blue peak leading to the particularly high quantum yield of this combination. However, if a different solvent or carboxylic acid is used, all three peaks are enhanced equally. More studies need to be done to explore this and consideration of the effect of the slight color imbalance would have to be weighed against the increase in quantum yield for a given application.

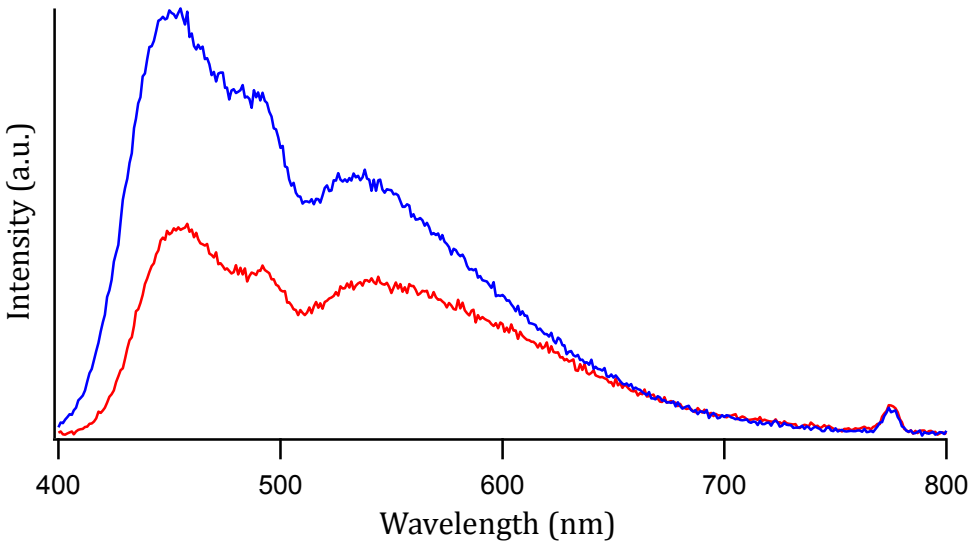

Figure 3.2. Example spectrum of a treatment done with hexanes as the nanocrystal solvent. The red spectrum is the emission spectrum of ultrasmall CdSe nanocrystals before treatment, and the blue spectrum is the emission spectrum of the same nanocrystals after treatment.

Table 3.3 summarizes the results of experiments investigating the effect of the reaction time of the treatment on different batches of nanocrystals. No conclusive trend in the quantum yield was observed for reaction times between 30 seconds and 35 minutes. For the times under 5 minutes in Table 3.3, aliquots were removed from the reaction vessel at the specified times as the nanocrystals were heated up to 60°C. Figures 3.3, 3.4, and 3.5 show fluorometry data of selected samples in which aliquots were removed at the specified times for a single treatment. The results of treatments on different batches of nanocrystals varied significantly. Figure 3.3 shows what one would expect as time progresses in a treatment, a growth in both the red and blue peaks with increasing time of the reaction. However, figure 3.4 shows no change in intensity or shape of the peaks as the treatment progressed. Figure 3.5 is particularly surprising; the aliquot taken

after just 30s has the highest quantum yield, and the peaks decayed over time as the treatment progressed. From Table 3.3, aliquots taken out after mixing the formic acid and nanocrystals for 30 s resulted in an average quantum yield of 29%. Interestingly, the reaction solution after mixing for 30 s had only heated to approximately 26°C at the time of aliquot removal. The significance of this is that one may not have to heat and stir for five minutes to do a formic acid treatment; similar results seem to be abtainable by simply mixing at room temperature for 30s. After taking the results on a case-by-case basis, it seemed that the red and blue peaks would grow over time and then reach a point in which they would start decaying. The time it would take to reach this point did not consistently follow any repeatable trend and seemed to be dependent on the nanocrystal batch and not on any treatment parameters. It should be noted that the time at which the blue peak would start decaying was often different from the time at which the red peak would start decaying suggesting two competing mechanisms.

Table 3.3. Reaction timing effects on resulting quantum yield.

Total time heated (min.)	Time Held at 60°C (min.)	Average Quantum Yield (%)	Standard Deviation (%)	Number of Trials
0.5	0	29	5	8
1.0	0	28	2	4
2.5	0	29	5	5
3.0	0	29	NA	1
3.5	0	22	NA	1
4.5	0	29	NA	1
5	0	28	4	9
7	0	23	NA	2
10	0	25	6	23
10	5	22	NA	1
15	5	17	NA	1
20	10	25	3	6
25	15	32	NA	1
30	20	24	6	7
35	25	27	NA	1

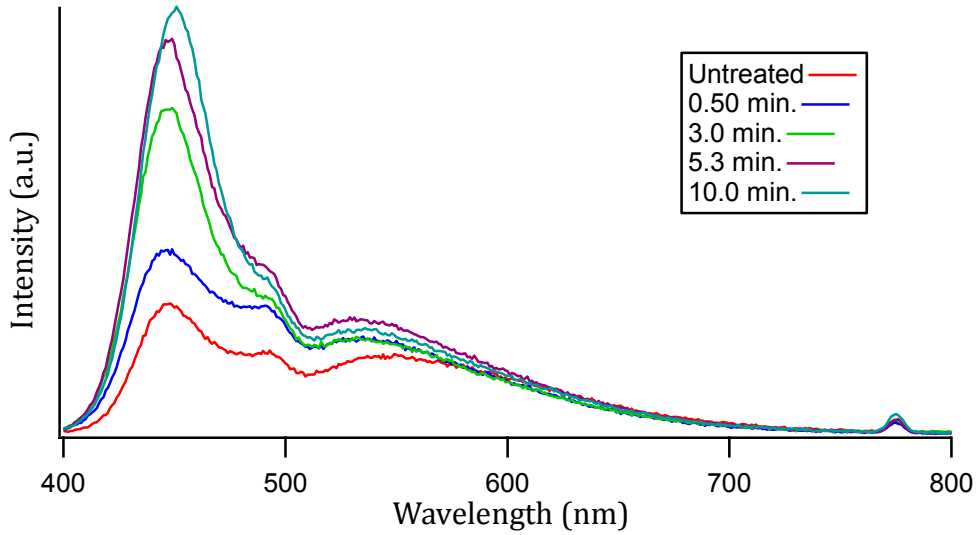

Figure 3.3. Spectra of aliquots taken from a treatment while it is progressing. The legend gives the quantum yield of the aliquot and the amount of time that the treatment was allowed to progress before an aliquot was taken out.

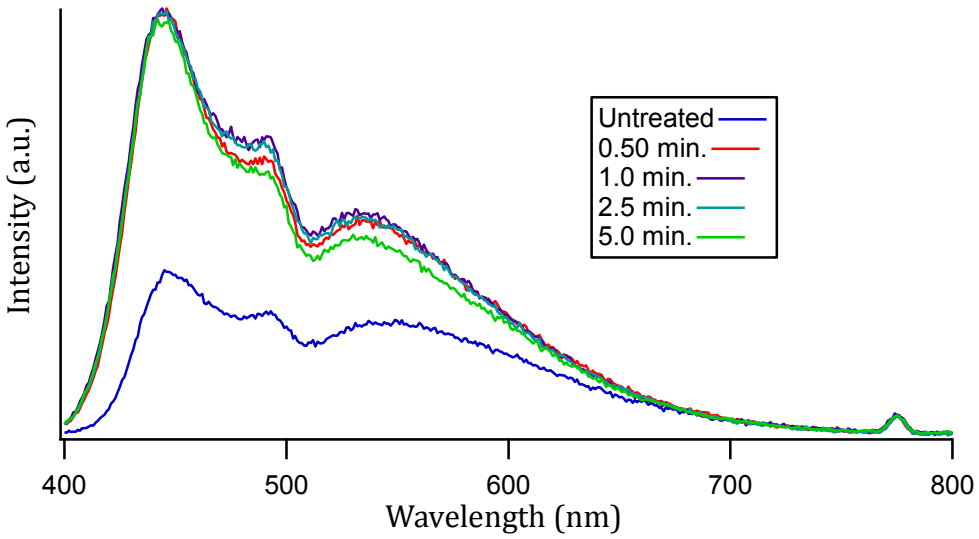

Figure 3.4. Spectra of aliquots taken from a treatment while it is progressing. The legend gives the quantum yield of the aliquot and the amount of time that the treatment was allowed to progress before an aliquot was taken out.

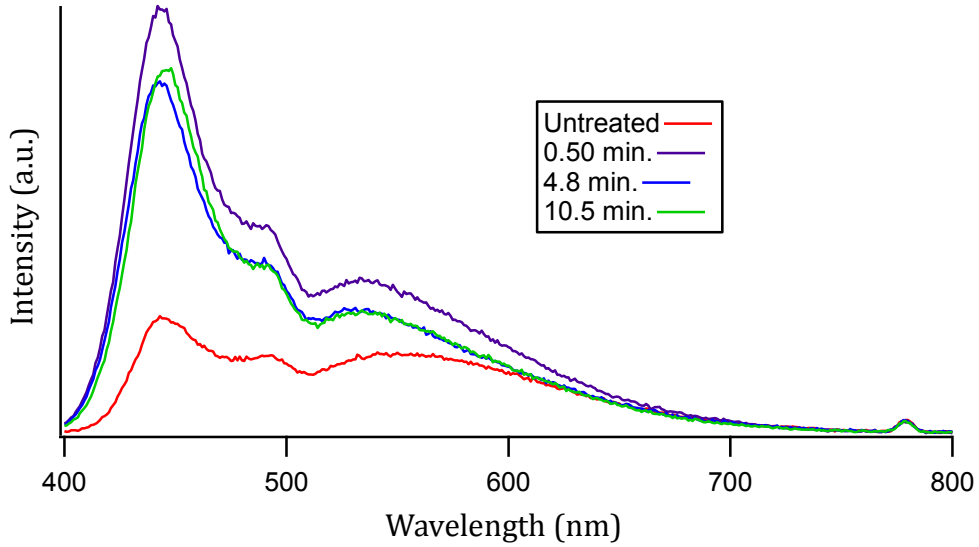

Figure 3.5. Spectra of aliquots taken from a treatment while it is progressing. The legend gives the quantum yield of the aliquot and the amount of time that the treatment was allowed to progress before an aliquot was taken out.

In order to investigate the resulting quantum yields of formic acid treatments performed without heating, room temperature treatments were carried out. Table 3.4 shows the time and resulting quantum yield for various room temperature treatment times. For each of these treatments, a treatment with heating was also done on the same batch. Overall, the treatments without heating did not result in as high a quantum yield as the treatments with heating. These results are confusing compared with the high quantum yields achieved with 30 s treatments. One possibility is that the best results that are obtained with room temperature treatments are obtained with short treatments. Another possibility is that as mentioned previously, the treatment is highly batch-dependent, so these results might reflect the batch of nanocrystals as opposed to the heating.

Table 3.4. Room temperature treatments.

Reaction Time (min.)	**Quantum Yield (%)**
10	19/22
20	23/15
30	26
90	18
180	18

Based on the prior results reported in this chapter, there is no clear correlation between many of the parameters of the formic acid treatment and the resulting quantum yield of the ultrasmall CdSe nanocrystal. The primary conclusion is that there is large variation in quantum yield after treatment from batch to batch of nanocrystals ranging from about 15% to 40%. The most promising hypothesis to explain these results is that the concentration of Se:TBP, which could be changing for different batches of nanocrystals, plays a key role in the resulting quantum yield

of the nanocrystals. If the injection volume is kept the same, the parameter that is being affected with changing concentration is the amount of Se being injected in the pot; another way to describe this is the anion to cation ratio. The reason for the variations in the concentration of the Se:TBP solution could be inconsistencies with measuring the weight of Se powder in the glove box. A more accurate balance was purchased in order to produce exact concentrations for these experiments.

Accordingly, the effect of the anion to cation ratio of the precursors for the synthesis of treated and untreated ultrasmall nanocrystals was explored. Kucur *et al.* found that higher photoluminescence for conventional nanocrystals could be obtained by increasing the Se:Cd ratio.[69] Qu *et al.* found that by using a high Se:Cd precursor ratio, higher quantum yields that lasted over longer reaction times were possible.[70] The effect of the Se:Cd raio was studied on the ultrasmall CdSe nanocrystals by changing the concentration of Se in a constant injection volume of tributylphosphine (TBP). Figure 3.6 shows the change in the intensity of the emission peaks of the ultrasmall nanocrystals with varying amounts of Se injected. When the Se:Cd ratio was modulated from 1.0:0.8 to 1.0:2.8, the untreated ultrasmall nanocrystal quantum yield increased from 9.0 to 15.3%, and the blue peak was enhanced giving a blue tint to the white light. For the treated nanocrystals, there was an optimum amount of Se at 2.4 mmol, and the white light for these nanocrystals also had more of a blue tint. All of the data points in Figure 3.6 are averaged data from at least three experiments for each concentration of Se.

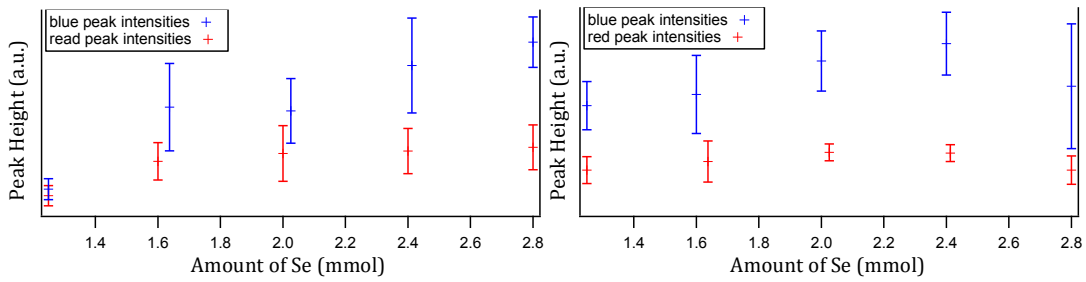

Figure 3.6. The effects of Se concentration on the emission intensities of the blue peak (blue points) and the red peak (red points) of untreated (left graph) and treated (right graph) ultrasmall nanocrystals. Each point represents an average of at least three different experiments.

In order to investigate whether the Se:Cd ratio was changing within the nanocrystal, preliminary RBS was performed on untreated ultrasmall and green-emitting CdSe nanocrystals using Se:TBP solutions with concentrations of 0.20 M, 0.40 M, and 0.70 M. Table 3.5 shows the Se to Cd ratios calculated using the results of these experiments. The green-emitting nanocrystals did not show a trend. However, the RBS suggests an increasing trend of Se:Cd can be seen with increasing precursor ratios of Se:Cd in ultrasmall nanocrystals, although there is some variation in the calculated Se:Cd ratio for similarly prepared samples. Part of this trend might be due to leftover precursors in the solution, so the exact ratios are still to be determined. In order to reduce noise, further RBS experiments need to be carried out with a higher concentration of nanocrystals on the graphene substrate before these results can be confirmed. Figure 3.7 shows the spectrum obtained from RBS of ultrasmall nanocrystals synthesized traditionally with 0.2 M Se:TBP (0.8 mmol).

Table 3.5. Se:Cd ratio determination of ultrasmall and green-emitting CdSe nanocrystals using different concentrations of Se:TBP by RBS

Nanocrystal Diameter	Amount of Se Precursor	Se:Cd Ratio
2.5 nm	0.8 mmol	1:1.2
2.5 nm	2.8 mmol	1:1.2
1.7 nm	0.8 mmol	1:1.7
1.7 nm	2.8 mmol	1:1.0
1.7 nm	2.8 mmol	1:0.60

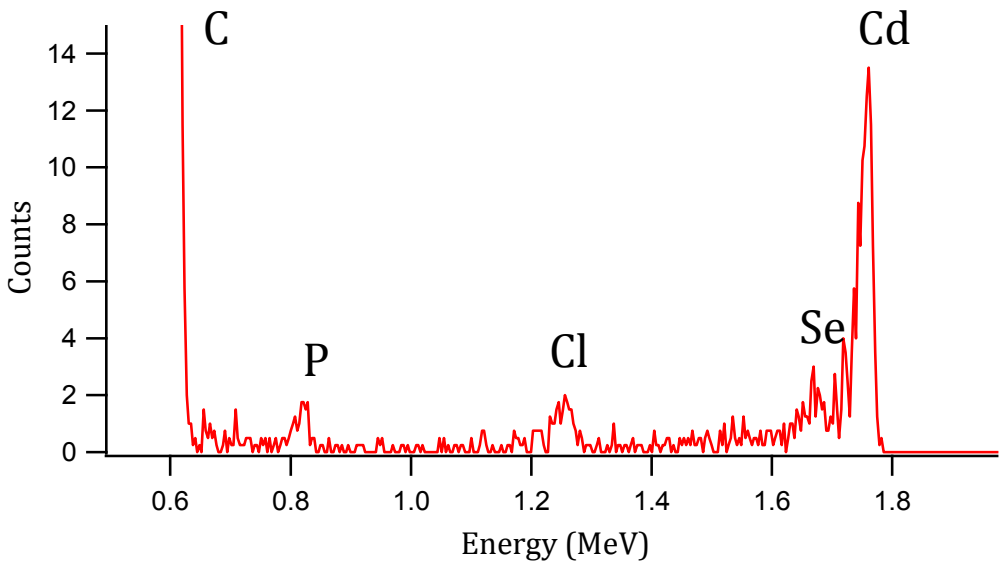

Figure 3.7. Example RBS spectrum of ultrasmall nanocrystals synthesized with a 0.2 M Se:TBP solution (0.8 mmol). The carbon, phosphorous, and chlorine peaks are from the graphene substrate, ligands of the nanocrystal, and cleaning of the substrate using chloroform, respectively.

It should be noted that during the course of the experiments performed with the formic acid treatment, it was found that the treatment was very sensitive to the environment of the nanocrystals after the treatment; if the condition of the solution after treatment was perturbed, the quantum yield could be affected. For example, if the solution after reaction was dried and then resolvated, the quantum yield of the nanocrystals decreased. Diluting the solution also lead to a decrease in nanocrystal

quantum yield. Figure 3.8 is an example of the emission of treated nanocrystals directly after treatment and emission of treated nanocrystals after being diluted for 2 days. Unlike the case in Figure 3.1 in which the quantum yield was enhanced 2 days after treatment, the quantum yield dropped significantly to the original quantum yield before the treatment. One interesting feature of this phenomenon is that the shape of the spectra between the sample taken directly after treatment and the sample that was diluted for 2 days is the same. Therefore, the nanocrystals do not go back to having their original, untreated properties after dilution. The shape of the spectra in Figure 3.1 also stayed the same regardless of increase of the fluorescence enhancement. This suggests that the treatment does have a permanent impact on the nanocrystal surface. More studies need to be done to identify what is happening to the surface during a treatment and what kind of effect the environment has on the surface.

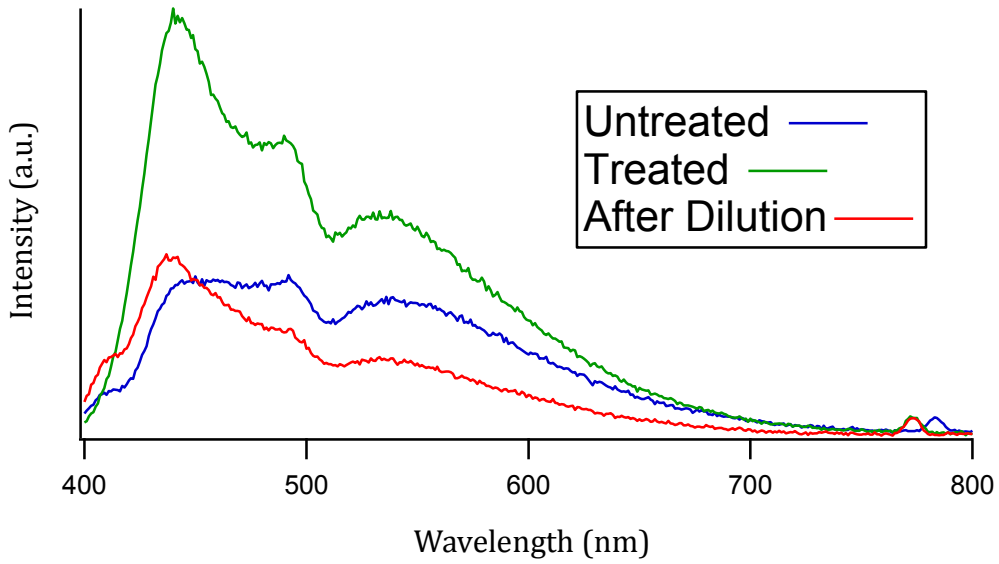

Figure 3.8. Example of fluorescent enhancement dependence on the reaction solution conditions. The blue spectrum is the spectrum of the original nanocrystals before treatment, and the green spectrum is the spectrum of the treated nanocrystals directly after treatment. After diluting the solution for 2 days, the fluorescent enhancement dropped (red spectrum).

3.2. Phosphor-based LEDs with Treated Nanocrystals.

The goal of attempting to improve the formic acid treatment was to be able to consistently achieve ~40% quantum yield for every treatment. With consistently higher quantum yields, incorporation of the ultrasmall nanocrystals into phosphor-based LEDs would lead to a reliably higher luminous efficacy of the white light LEDs. Although a consistently high quantum yield for the ultrasmall CdSe nanocrystals was not achieved, phosphor-based LEDs were made with selected batches of the treated nanocrystals that possessed quantum yields near 40%. For comparison, untreated nanocrystals were also encapsulated to form phosphor-based LEDs, and the difference in LED efficiency and color quality were investigated. Different weight percent (wt%) loadings were tried from 2 to 10%. With each wt% loading,

there was a trial and error process to figure out what amount of polymer and nanocrystal would give a particular thickness film. The thickness of the encapsulated nanocrystal film was reduced after curing, but the degree of reduction was not easily predictable. A thickness of about 50 μm was a starting goal because this thickness gave the brightest output without compromising the color quality for the devices that were made with untreated nanocrystals by Gosnell *et al.*[71] Schreuder *et al.* found that the color quality of the films did not change with weight loading and that the emission intensity of the films starts to plateau around 9 wt%.[60] However, Schreuder *et al.* measured the concentration of the ultrasmall nanocrystals by weighing a known volume of solution after it had dried. In this study, the concentration was measured using the UV-Vis and Yu *et al.* calculations, and the weight loading that gave the best results was 3 wt%.[67] However, more experiments need to be done to confirm this.

Most weight loadings above 3 wt% gave low efficiencies or were too dim to be detected with the spectrometer on the integrating sphere. This could be due to the extreme cloudiness of devices with high weight loadings. This cloudiness was likely caused by insufficient purification procedures in the ultrasmall nanocrystal synthesis. If a better purification method was found for the ultrasmall nanocrystal synthesis, brighter devices could be possible.

Table 3.6 gives average results of both treated and untreated ultrasmall nanocrystal device luminous efficacies at 2 and 3 wt% loadings. The main reason for the standard deviations was the amount of cloudiness of the device which was dependent upon the purity of the nanocrystals. The CIE coordinates and CRI did not

display a trend with weight loading and were (0.37 ± 0.05, 0.38 ± 0.05) and 90 ± 7, respectively, with 38 trials of both treated and untreated nanocrystals. As can be seen, there was a definite increase in efficacy with the wt% loading, but there was not a conclusive difference in the color quality or the efficacy when comparing treated and untreated nanocrystals. The lack of a difference in efficacies between treated and untreated nanocrystal devices could be due to the sensitivity of the treatment to its reaction solution. However, the accuracy of these results could be called into question because the spectrometer used with the integrating sphere was not sensitive enough to resolve the shape of the spectra of the films. An example spectrum is shown in Figure 3.9. Spikes of noise on the order of film emission were always present in these spectra, and the same spikes were often repeated from one spectrum to another. Additional experiments need to be done with a more sensitive spectrometer.

Table 3.6. Phosphor-based device efficacies at 2 and 3 wt% loadings.

Weight Loading (wt%)	**Average Untreated Efficiency (lm/W)**	**Standard Deviation (lm/W)**	**Number of Trials**	**Average Treated Efficiency (lm/W)**	**Standard Deviation (lm/W)**	**Number of Trials**
2	0.27	0.08	3	0.28	0.17	14
3	0.7	NA	1	0.50	0.12	5

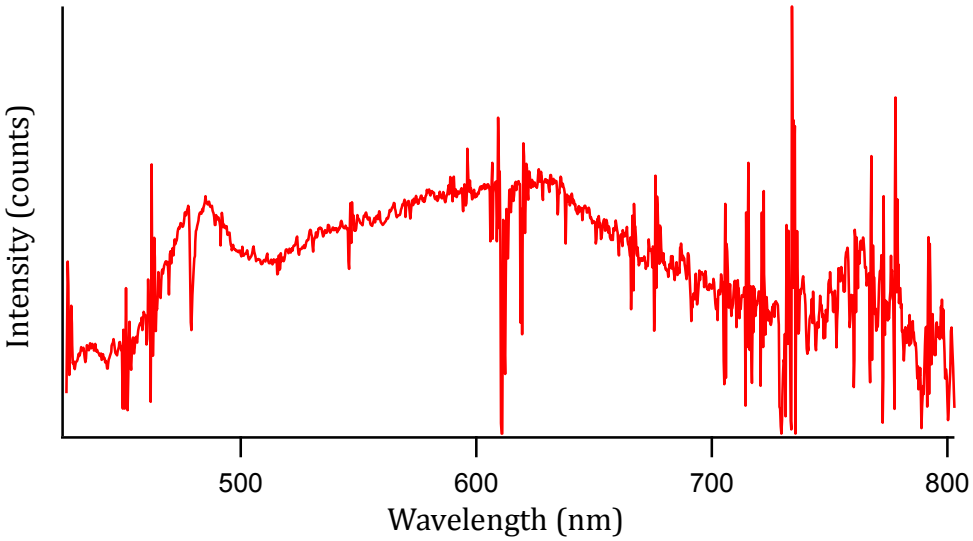

Figure 3.9. Example film spectrum from the CMS 500 Spectrometer connected to the integrating sphere

CHAPTER IV

CONCLUSIONS AND FUTURE DIRECTIONS

4.1 Possible Formic Acid Treatment Mechanism

All of the studies performed on the formic acid treatment provide insight into possible mechanisms. Within the ranges that were tested, the molar excess, concentration of the nanocrystal solution, and lighting environment (with the exception of UV light) did not have a large effect on the treatment. The fact that the treatment is not very dependent on the amounts of the formic acid and nanocrystals suggest that 30,000 is already a large enough excess for the treatment to work, and 15,000 molar excess might be sufficient to achieve the same results. Furthermore, since the reaction is not affected by visible light but is only affected by UV light, so an excited nanocrystal may not be as likely to be brightened.

The studies exploring the effect of the solvent in which the nanocrystals are susupended suggest that formic acid may only adhere to the surface of the nanocrystals if they are in a solvent in which the formic acid is immiscible. The solvents satisfying this criterion are toluene and mesitylene. One possibility is that the formic acid might be bonding very weakly to the surface through a secondary binding process like hydrogen bonding. This bonding would not be as likely if the formic acid prefers the environment of the solvent. The idea of a weak bonding mechanism is supported by the sensitivity of the solution after the treatment to its environment as shown in Figure 3.7.

The studies on the reaction time suggested two characteristics of the treatment. First, it seems as if there are two different mechanisms ocurring because the fluorescence enhancement of the red peak is not correlated with the fluorescence enhancement of the blue peak. Second, the treatment seems to be much more dependent on the particular batch of nanocrystals. This would make sense because many more parameters are involve in the synthesis of the nanocrystals compared with the treatment.

The experiments on the effects of the Se:Cd precursor ratio on treated and untreated ultrasmall nanocrystals show an increase in the quantum yield of nanocrystals before treatment with increasing Se:Cd precursor ratio and an optimum Se:Cd precursor ratio of 2.4:1 for high quantum yields after treatment. One can speculate whether this effect is caused by the production of a Se-rich surface by comparing it to other anion-rich surfaces that have been produced in the literature. Jasieniak *et al.* used successive ion layer adhesion and reaction (SILAR) in order to study the effects of differing surfaces of the nanocrystals, specifically a Cd-rich surface vs. a Se-rich surface.[72] Due to the lack of terminated bonds on surface Se atoms, the nanocrystal with a Se-rich surface exhibited severely quenched emission. However, it was found that the addition of TOP to these Se-rich nanocrystals which binds to Se surface atoms led to a brighter emission than the nanocrystals that were synthesized before the addition of the Se layer. Recently, Wei *et al.* used a similar method to modulate the photoluminescence of CdS nanocrystals; adding a S-rich surface quenched the photoluminescence and adding a Cd-rich surface on a S-rich surface completely replenished the photoluminescence.[73]

From these findings, it is doubtful that the surface of the ultrasmall nanocrystals are Se-rich with high Se:Cd precursor ratios; it is more likely that the surface of the nanocrystals approaches a 1:1 ratio of Se:Cd as the Se:Cd precursor ratio increases. The original ultrasmall nanocrystals involving a precursor ratio close to 1:1 (corresponding to a Se:TBP concentration of 0.2 M) might have vacant Se surface sites which could lead to surface Cd atoms that the bulky phosphonic acid cannot completely passivate.[61] By decreasing the number of Se vacancies, increasing the Se:Cd precursor ratio could be further passivating the nanocrystal. Considering that the shortest carboxylic acid increases the quantum yield the most with an emphasis on the blue peak, the formic acid could be squeezing into these vacant Se sites to passivate dangling Cd bonds that could otherwise lead to nonradiative emission. Along with hydrogen bonding, the cartoon in Figure 4.1 shows what this might look like. The red molecules are formic acid, and the long black chains are the ligands. As the Se:Cd ratio of precursors increases, the quantum yield of the untreated nanocrystals first increases but then starts to saturate as shown in Figure 3.5; this saturation could represent the point in which the Se:Cd ratio within the nanocrystal is approaching 1:1. Once most of the vacant Se surface sites are filled, the formic acid treatment would not be as effective which could explain the reason for the optimum Se:Cd ratio for the treatment.

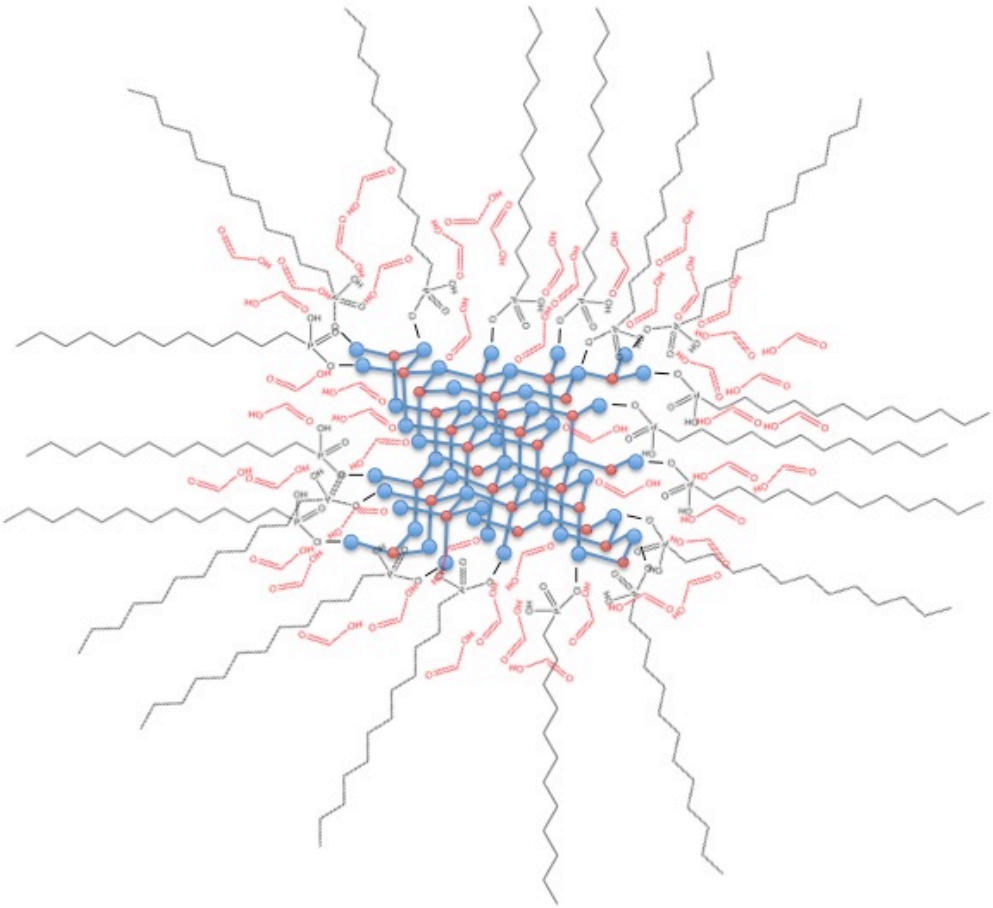

Figure 4.1. A cartoon of the proposed mechanism for the formic acid treatment that displays hydrogen bonding of the formic acid on the nanocrystal surface and the formic acid filling in Se vacancies.

The RBS results seem to confirm that there is an increase of the Se:Cd ratio within the nanocrystal with increasing Se:Cd precursor ratios. However, it is likely that this trend is partly due to lack of purification of the Se and Cd precursors. Many chomatographic methods could be used to analyze this possibility including high-pressure liquid chromatography and size-exclusion chromatography.[74-78] If the nanocrystals are not pure, these methods will give insight into how much of the trend is due to leftover precursors.

One promising method of characterizing ultrasmall nanocrystals is by solid-state nuclear magnetic resonance (SSNMR). Characterization of 2 nm CdSe nanocrystals was achieved for the first time by Berrettini *et al.* in 2004.[79] They were able to find the location of their ligands, thiophenol and hexadecylamine , on the nanocrystals. The thiophenol was far from surface Se atoms, and hexadecylamine (HDA) was close to surface Se atoms; they postulated that thiophenol was binding at Se vacancies, and the long HDA ligand which binds on surface Cd atoms tilts over the nanocrystal to achieve close proximity to surface Se atoms. If the same ligand characterization could be done with ultrasmall nanocrystals, this technique could give some insight into the mechanism of the formic acid treatment. SSNMR is also able to give valuable information on surface reconstruction and crystallinity of the nanocrystals because SSNMR selectively studies the surface of the nanocrystal instead of the nanomaterial as a whole. This could give more information on the fluxionality properties of ultrasmall nanocrystals.[80]

4.2 Ultrasmall Nanocrystal LEDs

Brighter phosphor-based LEDs with treated nanocrystals proved to be more of a challenge than expected. Devices made with higher weight loadings were particularly problematic due to cloudiness of the film. If a better method of purifying ultrasmall nanocrystals could be developed, more accurate results of the devices containing a higher weight loading of ultrasmall nanocrystals could be measured. Ultracentrifugation and size-exclusion chromatography are two methods that could be used to purify ultrasmall nanocrystals.[77, 81-83]

Other brightening methods for ultrasmall nanocrystal LEDs are possible. Many semiconductors are now being brightened using surface plasmon resonance (SPR) effects.[84-89] In order to effectively utilize SPR enhancement, the SPR wavelength must overlap with the emission of the semiconductor. Hence, for the broadband emission of the ultrasmall CdSe nanocrystals, a broad SPR is required to achieve uniform spectral brightening of the ultrasmall nanocrystals. Jiao *et al.* has fabricated a porous gold structure which displays a very broad, localized SPR centered at 500 nm.[90] This could be one option for brightening ultrasmall CdSe nanocrystals. In order to achieve this, one would have to deposit a thin layer of ultrasmall nanocrystals on the porous gold structure. Due to its ability to deposit even films on complex surfaces, electrophoretic deposition would be a viable candidate to attain an even deposition.[91-95]

Ultrasmall nanocrystals have been continually increasing in brightness since they were discovered in 2005 with an increase in quantum yield of ~20% with the formic acid treatment.[33, 39, 61] The objective of this thesis was to gain insights into the mechanism behind the formic acid treatment leading to more consistent nanocrystal quantum yields. While insights were gained, the treatment remains dependent on the reaction solution. With continued progress, it is expected that brightened, white light emitting, ultrasmall CdSe nanocrystals could be the foundation of cost-effective, high color quality white LEDs containing only one semiconductor.

APPENDIX A

LUMINOUS EFFICACY

The luminous efficacy of a light source is the amount of light that the average human eye perceives coming from the source divided by the electrical power that is put into the source.[2] This is different from the power efficiency which is the power of the light being emitted divided by the electrical power that is put into the source. Luminous efficacy is calculated as shown below in Equation A.1.

$$Luminous\ Efficacy = \eta_{LED} \times K \tag{A.1}$$

where η_{LED} is the power efficiency of the LED and K is the luminous efficacy of radiation of the test source.

The luminous efficacy of radiation is the amount of light that the human eye can perceive from a light source when one Watt of light is being emitted. At a given intensity of light, the human eye will perceive some wavelengths as brighter than others. Figure A.1 is a graph showing the relative brightness of different wavelengths to the human eye normalized to 1.[96] The human eye is most sensitive to green light, 555 nm to be exact. The maximum amount of lumens one can achieve from a 1 W source is 683 lm; in order to do this, the source would have to be a perfectly monochromatic light source at 555 nm. Therefore, in order to calculate the luminous efficacy of radiation, one assigns a level of importance to every

wavelength intensity in the source spectrum by integrating the luminosity function multiplied by the source spectrum. This integration multiplied by 683 lm/W and divided by the integrated luminosity function gives the luminous efficacy of radiation of a source, K. Another way to find K is by dividing the luminous intensity, $\emptyset_l$, of a source by its radiant intensity, $\emptyset_w$. See Equation A.2.

$$K = \frac{\emptyset_l}{\emptyset_w} = \frac{k_m \int_0^\infty P(\lambda)V(\lambda)d\lambda}{\int_0^\infty P(\lambda)d\lambda} \qquad (A.2)$$

k_m is 683 lm/W. $P(\lambda)$ is the luminosity function normalized so that the intensity at 555 nm is equal to one. $V(\lambda)$ is the fluorescence spectrum of the test source so that the maximum intensity is normalized to 1.

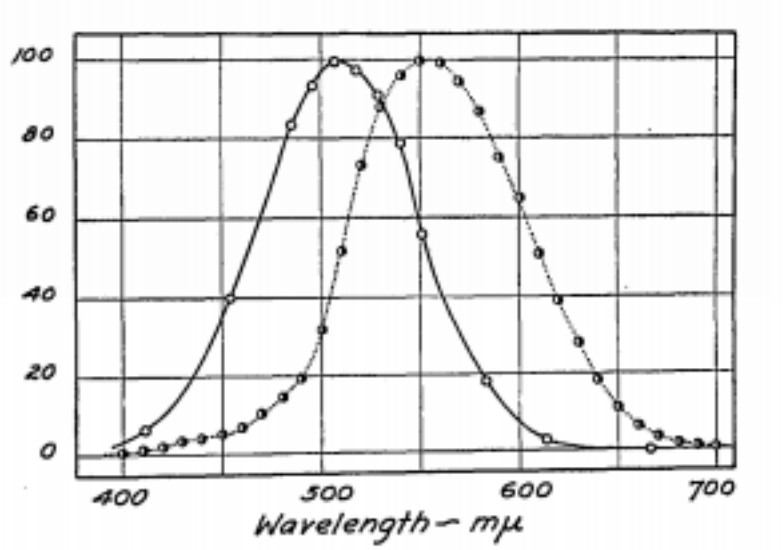

Figure A.1. The solid line is the luminosity function for scotopic vision, the sensitivity of the eye to visible wavelengths in low light. The dashed line is the luminosity function for photopic vision, the sensitivity of the eye to visible wavelengths in bright lighting.[96]

In the case of a phosphor-based device made with ultrasmall CdSe nanocrystals, the luminous efficacy is calculated as shown in Equations A.3 and A.4.[61]

$$Luminous\ Efficacy = \eta_{LED}\eta_{NC}\eta_{extrac} \times 250\frac{lm}{W} \qquad (A.3)$$

$$\eta_{NC} = \eta_{abs} \times QY \times S \qquad (A.4)$$

In the above equation, η_{LED} is the power efficiency of the excitation LED which in this work is a Nichia 385 nm UV LED with a power efficiency of 0.015. η_{NC}, the power efficiency of the nanocrystals, is the product of the percentage of photons absorbed by the nanocrystals from the excitation LED (η_{abs}), the quantum yield of the nanocrystals (QY), and the Stokes loss (S). In this work, $\eta_{abs} = 0.875$, and the stokes loss is approximately 0.750. The achievable value of QY is the subject of this thesis. η_{extrac} is the percentage of light emitted from the nanocrystals that escapes the device. In this work, light emitted through the encapsulating polymer film is equal to approximately 0.39. [97] The value of 250 lm/W in Equation A.3 is the calculated luminous efficacy of radiation for a typical spectrum of treated ultrasmall nanocrystals using Equation A.2; this constant converts the radiant flux (power of light in Watts) of the LED to luminous flux. The luminous efficacy achieved using nanocrystals with a quantum yield of 40% is 3.8 lm/W.[61]

APPENDIX B

CIE COORDINATES

CIE coordinates are a quantitative way to measure the color of light.[2] The calculation of CIE coordinates is based on three tristimulus values which are based on human cone cells in the human eye. There are three different types of human cone cells with responsivities at short (peaks at 420-440 nm), middle, (peaks at 530-540 nm) and long (peaks at 560-580 nm) wavelengths. One can think of the different types of cone cells as being the three primary colors; the mixture of the different levels of stimuli of each cone cell type can in theory give every possible color sensation. Similarly, CIE coordinates employ three color matching functions similar to the responsivities of the cone cells in human eyes as shown in Figure B.1.[98]

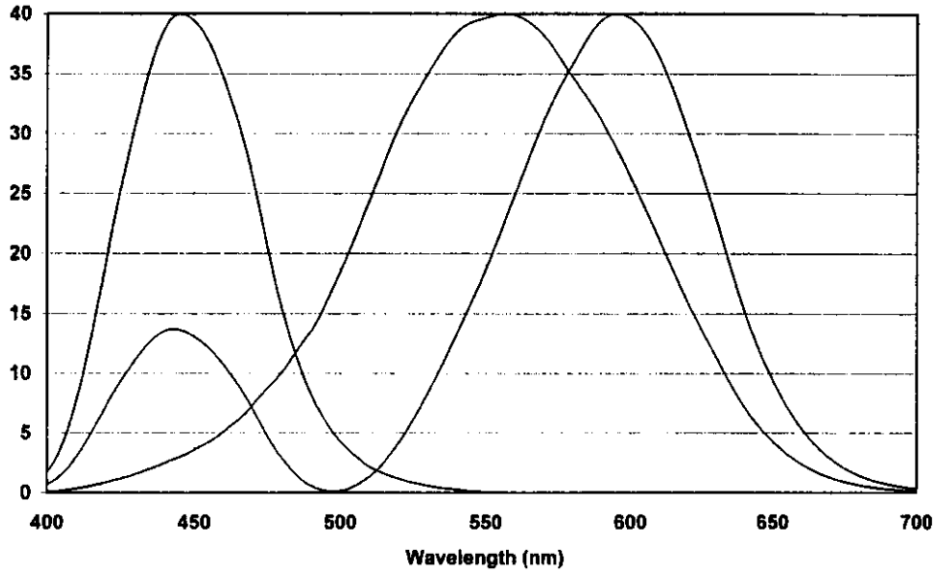

Figure B.1. Color matching functions that are used to calculate CIE coordinates, normalized to 40.[98]

The tristimulus values for the spectrum of the light source must first be calculated as shown in Equations B.1 through B.3.

$$X = \int_{380}^{780} I(\lambda)\, \bar{x}(\lambda) d\lambda \qquad (B.1)$$

$$Y = \int_{380}^{780} I(\lambda) \bar{y}(\lambda)\, d\lambda \qquad (B.2)$$

$$Z = \int_{380}^{780} I(\lambda) \bar{z}(\lambda) d\lambda \qquad (B.3)$$

$I(\lambda)$ is the source spectrum normalized to 1. $\bar{x}(\lambda)$, $\bar{y}(\lambda)$, and $\bar{z}(\lambda)$ are the three color matching functions shown in Figure B.1. Equations B.4 and B.5 show how to derive the CIE coordinates, (x, y). Figure B.2 shows the CIE coordinate color graph.[46]

$$x = \frac{X}{X + Y + Z} \tag{B.4}$$

$$y = \frac{Y}{X + Y + Z} \tag{B.5}$$

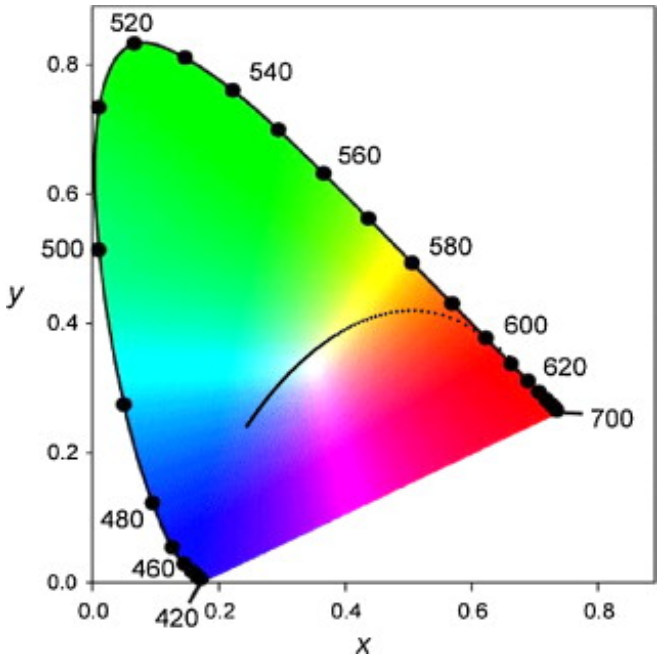

Figure B.2. CIE coordinates color graph where the black line is the Planckian locus.[46]

APPENDIX C

COLOR RENDERING INDEX

CRI is the ability of a light source to illuminate an object so that its color is perceived as the color of the same object when illuminated by sunlight. CRI ranges from -100 for a poor light source to 100 for an excellent light source.[2] The CRI is measured by comparing the reflection off many different samples under a reference source whose CRI approaches 100 and the test source. In order to calculate CRI, one must first make sure that the CIE coordinates of the emitted light of the test source is less than 5.4×10^{-3} away from the Planckian locus in the CIE chart. This is done using Equation C.1 where u_t and v_t are the CIE coordinates of the light being emitted from the test source and u_r and v_r are the coordinates on the Planckian locus that are closest to u_t and v_t.

$$DC = \sqrt{(u_r - u_t)^2 + (v_r - v_t)^2} < 5.4\times10^{-3} \qquad (C.1)$$

Next one uses the von Kries chromatic transform equation to find the corresponding color for each sample. This is done using Equations $C.2$ through $C.5$ where c and d are found for test and reference sources first. Then, $u_{c,i}$ and $v_{c,i}$ give the corresponding color for each sample.

$$c = \frac{(4.0 - u - 10.0v)}{v} \tag{C.2}$$

$$d = \frac{(1.780v - 1.481u + 0.404)}{v} \tag{C.3}$$

$$u_{c,i} = \frac{10.872 + 0.404\left(\frac{c_r}{c_t}\right)c_{t,i} - 4\left(\frac{d_r}{d_t}\right)d_{t,i}}{16.518 + 1.481\left(\frac{c_r}{c_t}\right)c_{t,i} - \left(\frac{d_r}{d_t}\right)d_{t,i}} \tag{C.4}$$

$$v_{c,i} = \frac{5.520}{16.528 + 1.481\left(\frac{c_r}{c_t}\right)c_{t,i} - \left(\frac{d_r}{d_t}\right)d_{t,i}} \tag{C.5}$$

where the subscripts r and t stand for reference and test source respectively. $c_{t,i}$ and $d_{t,i}$ come from the inner product of the test illuminant and the spectral reflectivity of sample i.

Next, one calculates the rendering index, R_i, for each sample using Equation C.6

$$R_i = 100 - 4.6\Delta E_i \tag{C.6}$$

where ΔE_i is the Euclidean distance between the CIE coordinates of the reflectivity of the object with the test source and the CIE coordinates of the reflectivity of the object with the reference source. CRI is calculated by taking the arithmetic mean of all R_i.

REFERENCES

1. Humphreys, C. J., Solid-State Lighting. *MRS Bulletin* **2008,** *33* (04), 459-470 M3 - 10.1557/mrs2008.91.

2. Zukauskas, A.; Shur, M. S.; Caska, R., *Introduction to Solid State Lighting*. John Wiley & Sons, Inc.: New York, 2002.

3. Light's Labour's Lost: Policies for Energy-efficient Lighting. International Energy Agency: Paris, France.

4. Energy Savings Potential of Solid-state Lighting in General Illumination Applications. U.S. Department of Energy: 2012.

5. Phase Out of Incandescent Lamps: Implications for International Supply and Demand for Regulatory Compliant Lamps. International Energy Agency: Paris, France, 2010.

6. Solid-state Lighting Research and Development: Manufacturing Roadmap. U.S. Department of Energy: 2012.

7. Taguchi, T., Present Status of Energy Saving Technologies and Future Prospect in White LED Lighting. *IEEJ Transactions on Electrical and Electronic Engineering* **2008,** *3* (1), 21-26.

8. Rosenthal, S. J.; McBride, J.; Pennycook, S. J.; Feldman, L. C., Synthesis, surface studies, composition and structural characterization of CdSe, core/shell and biologically active nanocrystals. *Surface Science Reports* **2007,** *62* (4), 111-157.

9. Anikeeva, P. O.; Halpert, J. E.; Bawendi, M. G.; Bulović, V., Electroluminescence from a Mixed Red−Green−Blue Colloidal Quantum Dot Monolayer. *Nano Letters* **2007,** *7* (8), 2196-2200.

10. Achermann, M.; Petruska, M. A.; Kos, S.; Smith, D. L.; Koleske, D. D.; Klimov, V. I., Energy-transfer pumping of semiconductor nanocrystals using an epitaxial quantum well. *Nature* **2004,** *429* (6992), 642-646.

11. Dabbousi, B. O.; Bawendi, M. G.; Onitsuka, O.; Rubner, M. F., Electroluminescence from CdSe quantum-dot/polymer composites. *Applied Physics Letters* **1995,** *66* (11), 1316-1318.

12. Coe, S.; Woo, W.-K.; Bawendi, M.; Bulovic, V., Electroluminescence from single monolayers of nanocrystals in molecular organic devices. *Nature* **2002,** *420* (6917), 800-803.

13. Hetsch, F.; Xu, X.; Wang, H.; Kershaw, S. V.; Rogach, A. L., Semiconductor Nanocrystal Quantum Dots as Solar Cell Components and Photosensitizers: Material, Charge Transfer, and Separation Aspects of Some Device Topologies. *The Journal of Physical Chemistry Letters* **2011,** *2* (15), 1879-1887.

14. Kramer, I. J.; Sargent, E. H., Colloidal Quantum Dot Photovoltaics: A Path Forward. *ACS Nano* **2011,** *5* (11), 8506-8514.

15. Chang, J. C.; Tomlinson, I. D.; Warnement, M. R.; Ustione, A.; Carneiro, A. M. D.; Piston, D. W.; Blakely, R. D.; Rosenthal, S. J., Single Molecule Analysis of Serotonin Transporter Regulation Using Antagonist-Conjugated Quantum Dots Reveals Restricted, p38 MAPK-Dependent Mobilization Underlying Uptake Activation. *The Journal of Neuroscience* **2012,** *32* (26), 8919-8929.

16. Alivisatos, P., The use of nanocrystals in biological detection. *Nat Biotech* **2004,** *22* (1), 47-52.

17. Michalet, X.; Pinaud, F. F.; Bentolila, L. A.; Tsay, J. M.; Doose, S.; Li, J. J.; Sundaresan, G.; Wu, A. M.; Gambhir, S. S.; Weiss, S., Quantum Dots for Live Cells, in Vivo Imaging, and Diagnostics. *Science* **2005,** *307* (5709), 538-544.

18. Howarth, M.; Liu, W.; Puthenveetil, S.; Zheng, Y.; Marshall, L. F.; Schmidt, M. M.; Wittrup, K. D.; Bawendi, M. G.; Ting, A. Y., Monovalent, reduced-size quantum dots for imaging receptors on living cells. *Nat Meth* **2008,** *5* (5), 397-399.

19. Dahan, M.; Lévi, S.; Luccardini, C.; Rostaing, P.; Riveau, B.; Triller, A., Diffusion Dynamics of Glycine Receptors Revealed by Single-Quantum Dot Tracking. *Science* **2003,** *302* (5644), 442-445.

20. Rosenthal, S. J.; Tomlinson, I.; Adkins, E. M.; Schroeter, S.; Adams, S.; Swafford, L.; McBride, J.; Wang, Y.; DeFelice, L. J.; Blakely, R. D., Targeting Cell Surface Receptors with Ligand-Conjugated Nanocrystals. *Journal of the American Chemical Society* **2002,** *124* (17), 4586-4594.

21. Murray, C. B.; Norris, D. J.; Bawendi, M. G., Synthesis and characterization of nearly monodisperse CdE (E = sulfur, selenium, tellurium) semiconductor nanocrystallites. *Journal of the American Chemical Society* **1993,** *115* (19), 8706-8715.

22. Landes, C.; Braun, M.; Burda, C.; El-Sayed, M. A., Observation of Large Changes in the Band Gap Absorption Energy of Small CdSe Nanoparticles Induced by the Adsorption of a Strong Hole Acceptor. *Nano Letters* **2001,** *1* (11), 667-670.

23. Peng, Z. A.; Peng, X., Formation of High-Quality CdTe, CdSe, and CdS Nanocrystals Using CdO as Precursor. *Journal of the American Chemical Society* **2000,** *123* (1), 183-184.

24. Peng, Z. A.; Peng, X., Nearly Monodisperse and Shape-Controlled CdSe Nanocrystals via Alternative Routes: Nucleation and Growth. *Journal of the American Chemical Society* **2002,** *124* (13), 3343-3353.

25. Qu, L.; Peng, Z. A.; Peng, X., Alternative Routes toward High Quality CdSe Nanocrystals. *Nano Letters* **2001,** *1* (6), 333-337.

26. Cumberland, S. L.; Hanif, K. M.; Javier, A.; Khitrov, G. A.; Strouse, G. F.; Woessner, S. M.; Yun, C. S., Inorganic Clusters as Single-Source Precursors for Preparation of CdSe, ZnSe, and CdSe/ZnS Nanomaterials. *Chemistry of Materials* **2002,** *14* (4), 1576-1584.

27. Qu, L.; Yu, W. W.; Peng, X., In Situ Observation of the Nucleation and Growth of CdSe Nanocrystals. *Nano Letters* **2004,** *4* (3), 465-469.

28. Kudera, S.; Zanella, M.; Giannini, C.; Rizzo, A.; Li, Y.; Gigli, G.; Cingolani, R.; Ciccarella, G.; Spahl, W.; Parak, W. J.; Manna, L., Sequential Growth of Magic-Size CdSe Nanocrystals. *Advanced Materials* **2007,** *19* (4), 548-552.

29. Cossairt, B. M.; Owen, J. S., CdSe Clusters: At the Interface of Small Molecules and Quantum Dots. *Chemistry of Materials* **2011,** *23* (12), 3114-3119.

30. Beri, R. K.; Khanna, P. K., "Green" and controlled synthesis of single family "magic-size" cadmium selenide nanocrystals by the use of cyclo-hexeno-1,2,3-selenadiazole an organoselenium compound. *CrystEngComm* **2010,** *12* (10), 2762-2768.

31. Ouyang, J.; Zaman, M. B.; Yan, F. J.; Johnston, D.; Li, G.; Wu, X.; Leek, D.; Ratcliffe, C. I.; Ripmeester, J. A.; Yu, K., Multiple Families of Magic-Sized CdSe Nanocrystals with Strong Bandgap Photoluminescence via Noninjection One-Pot Syntheses. *The Journal of Physical Chemistry C* **2008,** *112* (36), 13805-13811.

32. Yu, K.; Hu, M. Z.; Wang, R.; Piolet, M. l. L.; Frotey, M.; Zaman, M. B.; Wu, X.; Leek, D. M.; Tao, Y.; Wilkinson, D.; Li, C., Thermodynamic Equilibrium-Driven Formation of Single-Sized Nanocrystals: Reaction Media Tuning CdSe Magic-Sized versus Regular Quantum Dots. *The Journal of Physical Chemistry C* **2010,** *114* (8), 3329-3339.

33. Bowers, M. J.; McBride, J. R.; Rosenthal, S. J., White-Light Emission from Magic-Sized Cadmium Selenide Nanocrystals. *Journal of the American Chemical Society* **2005,** *127* (44), 15378-15379.

34. Dukes, A. D.; McBride, J. R.; Rosenthal, S. J., Synthesis of Magic-Sized CdSe and CdTe Nanocrystals with Diisooctylphosphinic Acid. *Chemistry of Materials* **2010,** *22* (23), 6402-6408.

35. Cossairt, B. M.; Juhas, P.; Billinge, S. J. L.; Owen, J. S., Tuning the Surface Structure and Optical Properties of CdSe Clusters Using Coordination Chemistry. *The Journal of Physical Chemistry Letters* **2011,** *2* (24), 3075-3080.

36. Yu, K., CdSe Magic-Sized Nuclei, Magic-Sized Nanoclusters and Regular Nanocrystals: Monomer Effects on Nucleation and Growth. *Advanced Materials* **2012,** *24* (8), 1123-1132.

37. Shen, C.-C.; Tseng, W.-L., One-Step Synthesis of White-Light-Emitting Quantum Dots at Low Temperature. *Inorganic Chemistry* **2009,** *48* (18), 8689-8694.

38. Jose, R.; Zhelev, Z.; Bakalova, R.; Baba, Y.; Ishikawa, M., White-light-emitting CdSe quantum dots synthesized at room temperature. *Applied Physics Letters* **2006,** *89* (1), 013115-3.

39. Schreuder, M. A.; McBride, J. R.; Dukes, A. D.; Sammons, J. A.; Rosenthal, S. J., Control of Surface State Emission via Phosphonic Acid Modulation in Ultrasmall CdSe Nanocrystals: The Role of Ligand Electronegativity. *The Journal of Physical Chemistry C* **2009,** *113* (19), 8169-8176.

40. Bowers Ii, M. J.; McBride, J. R.; Garrett, M. D.; Sammons, J. A.; Dukes Iii, A. D.; Schreuder, M. A.; Watt, T. L.; Lupini, A. R.; Pennycook, S. J.; Rosenthal, S. J., Structure and Ultrafast Dynamics of White-Light-Emitting CdSe Nanocrystals. *Journal of the American Chemical Society* **2009,** *131* (16), 5730-5731.

41. Dukes, A. D.; Iii; Schreuder, M. A.; Sammons, J. A.; McBride, J. R.; Smith, N. J.; Rosenthal, S. J., Pinned emission from ultrasmall cadmium selenide nanocrystals. *The Journal of Chemical Physics* **2008,** *129* (12), 121102-4.

42. Liu, Y.-H.; Wang, F.; Wang, Y.; Gibbons, P. C.; Buhro, W. E., Lamellar Assembly of Cadmium Selenide Nanoclusters into Quantum Belts. *Journal of the American Chemical Society* **2011,** *133* (42), 17005-17013.

43. Jose, R.; Zhanpeisov, N. U.; Fukumura, H.; Baba, Y.; Ishikawa, M., Structure−Property Correlation of CdSe Clusters Using Experimental Results and First-Principles DFT Calculations. *Journal of the American Chemical Society* **2005,** *128* (2), 629-636.

44. Chen, X.; Samia, A. C. S.; Lou, Y.; Burda, C., Investigation of the Crystallization Process in 2 nm CdSe Quantum Dots. *Journal of the American Chemical Society* **2005,** *127* (12), 4372-4375.

45. Owen, J. S.; Chan, E. M.; Liu, H.; Alivisatos, A. P., Precursor Conversion Kinetics and the Nucleation of Cadmium Selenide Nanocrystals. *Journal of the American Chemical Society* **2010,** *132* (51), 18206-18213.

46. Demir, H. V.; Nizamoglu, S.; Erdem, T.; Mutlugun, E.; Gaponik, N.; Eychmüller, A., Quantum dot integrated LEDs using photonic and excitonic color conversion. *Nano Today* **2011**.

47. Anikeeva, P. O.; Halpert, J. E.; Bawendi, M. G.; Bulovic, V., Electroluminescence from a mixed red-green-blue colloidal quantum dot monolayer. *Nano Letters* **2007,** *7* (8), 2196-2200.

48. Tan, Z.; Hedrick, B.; Zhang, F.; Zhu, T.; Xu, J.; Henderson, R. H.; Ruzyllo, J.; Wang, A. Y., Stable binary complementary white light-emitting diodes based on quantum-dot/polymer-bilayer structures. *Photonics Technology Letters, IEEE* **2008,** *20* (23), 1998-2000.

49. Li, Y. Q.; Rizzo, A.; Cingolani, R.; Gigli, G., Bright White‐Light‐Emitting Device from Ternary Nanocrystal Composites. *Advanced materials* **2006,** *18* (19), 2545-2548.

50. Kim, L.; Anikeeva, P. O.; Coe-Sullivan, S. A.; Steckel, J. S.; Bawendi, M. G.; Bulovic, V., Contact printing of quantum dot light-emitting devices. *Nano letters* **2008,** *8* (12), 4513-4517.

51. Woo, J. Y.; Kim, K.; Jeong, S.; Han, C.-S., Enhanced Photoluminance of Layered Quantum Dot–Phosphor Nanocomposites as Converting Materials for Light Emitting Diodes. *The Journal of Physical Chemistry C* **2011,** *115* (43), 20945-20952.

52. Ziegler, J.; Xu, S.; Kucur, E.; Meister, F.; Batentschuk, M.; Gindele, F.; Nann, T., Silica-Coated InP/ZnS Nanocrystals as Converter Material in White LEDs. *Advanced Materials* **2008,** *20* (21), 4068-4073.

53. Jang, H. S.; Yang, H.; Kim, S. W.; Han, J. Y.; Lee, S.-G.; Jeon, D. Y., White Light-Emitting Diodes with Excellent Color Rendering Based on Organically Capped CdSe Quantum Dots and Sr3SiO5:Ce3+,Li+ Phosphors. *Advanced Materials* **2008,** *20* (14), 2696-2702.

54. Nizamoglu, S.; Ozel, T.; Sari, E.; Demir, H. V., White light generation using CdSe/ZnS core–shell nanocrystals hybridized with InGaN/GaN light emitting diodes. *Nanotechnology* **2007,** *18* (6), 065709.

55. Chen, H.-S.; Cheng-Kuo, H.; Hong, H.-Y., InGaN-CdSe-ZnSe quantum dots white LEDs. *Photonics Technology Letters, IEEE* **2006,** *18* (1), 193-195.

56. Nizamoglu, S.; Mutlugun, E.; Ozel, T.; Demir, H. V.; Sapra, S.; Gaponik, N.; Eychmuller, A., Dual-color emitting quantum-dot-quantum-well CdSe-ZnS heteronanocrystals hybridized on InGaN/GaN light emitting diodes for high-quality white light generation. *Applied Physics Letters* **2008,** *92* (11), 113110-3.

57. Schreuder, M. A.; Xiao, K.; Ivanov, I. N.; Weiss, S. M.; Rosenthal, S. J., White Light-Emitting Diodes Based on Ultrasmall CdSe Nanocrystal Electroluminescence. *Nano Letters* **2010,** *10* (2), 573-576.

58. Nizamoglu, S.; Demir, H. V., Resonant nonradiative energy transfer in CdSe/ZnS core/shell nanocrystal solids enhances hybrid white light emitting diodes. *Optics Express* **2008,** *16* (18), 13961-13968.

59. Nizamoglu, S.; Mutlugun, E.; Akyuz, O.; Perkgoz, N. K.; Demir, H. V.; Liebscher, L.; Sapra, S.; Gaponik, N.; Eychmüller, A., White emitting CdS quantum dot nanoluminophores hybridized on near-ultraviolet LEDs for high-quality white light generation and tuning. *New Journal of Physics* **2008,** *10* (2), 023026.

60. Schreuder, M. A.; Gosnell, J. D.; Smith, N. J.; Warnement, M. R.; Weiss, S. M.; Rosenthal, S. J., Encapsulated white-light CdSe nanocrystals as nanophosphors for solid-state lighting. *Journal of Materials Chemistry* **2008,** *18* (9), 970-975.

61. Rosson, T. E.; Claiborne, S. M.; McBride, J. R.; Stratton, B. S.; Rosenthal, S. J., Bright White Light Emission from Ultrasmall Cadmium Selenide Nanocrystals. *Journal of the American Chemical Society* **2012,** *134* (19), 8006-8009.

62. Mekis, I.; Talapin, D. V.; Kornowski, A.; Haase, M.; Weller, H., One-Pot Synthesis of Highly Luminescent CdSe/CdS Core−Shell Nanocrystals via Organometallic and "Greener" Chemical Approaches†. *The Journal of Physical Chemistry B* **2003,** *107* (30), 7454-7462.

63. Peng, X.; Schlamp, M. C.; Kadavanich, A. V.; Alivisatos, A. P., Epitaxial Growth of Highly Luminescent CdSe/CdS Core/Shell Nanocrystals with Photostability and Electronic Accessibility. *Journal of the American Chemical Society* **1997,** *119* (30), 7019-7029.

64. Dabbousi, B. O.; Rodriguez-Viejo, J.; Mikulec, F. V.; Heine, J. R.; Mattoussi, H.; Ober, R.; Jensen, K. F.; Bawendi, M. G., (CdSe)ZnS Core−Shell Quantum Dots: Synthesis and Characterization of a Size Series of Highly Luminescent Nanocrystallites. *The Journal of Physical Chemistry B* **1997,** *101* (46), 9463-9475.

65. Chen, X.; Lou, Y.; Samia, A. C.; Burda, C., Coherency Strain Effects on the Optical Response of Core/Shell Heteronanostructures. *Nano Letters* **2003,** *3* (6), 799-803.

66. Rosson, T. E., Fluorescence Enhancement of White-light Cadmium Selenide Nanocrystals. Vanderbilt University: Nashville, TN, 2011.

67. Yu, W. W.; Qu, L.; Guo, W.; Peng, X., Experimental Determination of the Extinction Coefficient of CdTe, CdSe, and CdS Nanocrystals. *Chemistry of Materials* **2003,** *15* (14), 2854-2860.

68. Reynolds, G. A.; Drexhage, K. H., New coumarin dyes with rigidized structure for flashlamp-pumped dye lasers. *Optics Communications* **1975,** *13* (3), 222-225.

69. Kuçur, E.; Ziegler, J.; Nann, T., Synthesis and Spectroscopic Characterization of Fluorescent Blue-Emitting Ultrastable CdSe Clusters. *Small* **2008,** *4* (7), 883-887.

70. Qu, L.; Peng, X., Control of Photoluminescence Properties of CdSe Nanocrystals in Growth. *Journal of the American Chemical Society* **2002,** *124* (9), 2049-2055.

71. Gosnell, J. D.; Rosenthal, S. J.; Weiss, S. M., White Light Emission Characteristics of Polymer-Encapsulated CdSe Nanocrystal Films. *Photonics Technology Letters, IEEE* **2010,** *22* (8), 541-543.

72. Jasieniak, J.; Mulvaney, P., From Cd-Rich to Se-Rich – the Manipulation of CdSe Nanocrystal Surface Stoichiometry. *Journal of the American Chemical Society* **2007,** *129* (10), 2841-2848.

73. Wei, H. H.-Y.; Evans, C. M.; Swartz, B. D.; Neukirch, A. J.; Young, J.; Prezhdo, O. V.; Krauss, T. D., Colloidal Semiconductor Quantum Dots with Tunable Surface Composition. *Nano Letters* **2012,** *12* (9), 4465-4471.

74. Pinaud, F.; King, D.; Moore, H.-P.; Weiss, S., Bioactivation and cell targeting of semiconductor CdSe/ZnS nanocrystals with phytochelatin-related peptides. *Journal of the American Chemical Society* **2004,** *126* (19), 6115-6123.

75. Wilson, W. L.; Szajowski, P. F.; Brus, L. E., Quantum confinement in size-selected, surface-oxidized silicon nanocrystals. *SCIENCE-NEW YORK THEN WASHINGTON*- **1993,** *262*, 1242-1242.

76. Fortner, J. D.; Lyon, D. Y.; Sayes, C. M.; Boyd, A. M.; Falkner, J. C.; Hotze, E. M.; Alemany, L. B.; Tao, Y. J.; Guo, W.; Ausman, K. D., C60 in water: nanocrystal formation and microbial response. *Environmental science & technology* **2005,** *39* (11), 4307-4316.

77. Ali, M.; Krueger, K. M.; Falkner, J. C.; Colvin, V. L., Recycling size exclusion chromatography for the analysis and separation of nanocrystalline gold. *Analytical chemistry* **2004,** *76* (19), 5903-5910.

78. Krueger, K. M.; Ali, M.; Falkner, J. C.; Colvin, V. L., Characterization of nanocrystalline CdSe by size exclusion chromatography. *Analytical chemistry* **2005,** *77* (11), 3511-3515.

79. Berrettini, M. G.; Braun, G.; Hu, J. G.; Strouse, G. F., NMR Analysis of Surfaces and Interfaces in 2-nm CdSe. *Journal of the American Chemical Society* **2004,** *126* (22), 7063-7070.

80. Pennycook, T. J.; McBride, J. R.; Rosenthal, S. J.; Pennycook, S. J.; Pantelides, S. T., Dynamic Fluctuations in Ultrasmall Nanocrystals Induce White Light Emission. *Nano Letters* **2012,** *12* (6), 3038-3042.

81. Ellery, W. N.; Schleyer, M. H., Comparison of homogenization and ultrasonication as techniques in extracting attached sedimentary bacteria. *Marine ecology progress series. Oldendorf* **1984,** *15* (3), 247-250.

82. Shah, S.; Sharma, A.; Gupta, M. N., Extraction of oil from Jatropha curcas L. seed kernels by combination of ultrasonication and aqueous enzymatic oil extraction. *Bioresource Technology* **2005,** *96* (1), 121-123.

83. Carion, O.; Mahler, B.; Pons, T.; Dubertret, B., Synthesis, encapsulation, purification and coupling of single quantum dots in phospholipid micelles for their use in cellular and in vivo imaging. *Nature Protocols* **2007,** *2* (10), 2383-2390.

84. Eustis, S.; El-Sayed, M. A., Why gold nanoparticles are more precious than pretty gold: Noble metal surface plasmon resonance and its enhancement of the radiative and nonradiative properties of nanocrystals of different shapes. *Chemical Society Reviews* **2006,** *35* (3), 209-217.

85. Mohamed, M. B.; Volkov, V.; Link, S.; El-Sayed, M. A., The `lightning' gold nanorods: fluorescence enhancement of over a million compared to the gold metal. *Chemical Physics Letters* **2000,** *317* (6), 517-523.

86. Song, J.-H.; Atay, T.; Shi, S.; Urabe, H.; Nurmikko, A. V., Large Enhancement of Fluorescence Efficiency from CdSe/ZnS Quantum Dots Induced by Resonant Coupling to Spatially Controlled Surface Plasmons. *Nano Letters* **2005,** *5* (8), 1557-1561.

87. Tam, F.; Goodrich, G. P.; Johnson, B. R.; Halas, N. J., Plasmonic Enhancement of Molecular Fluorescence. *Nano Letters* **2007,** *7* (2), 496-501.

88. Hayakawa, T.; Selvan, S. T.; Nogami, M., Field enhancement effect of small Ag particles on the fluorescence from Eu^{3+}-doped SiO_2 glass. *Applied Physics Letters* **1999,** *74* (11), 1513-1515.

89. Shimizu, K. T.; Woo, W. K.; Fisher, B. R.; Eisler, H. J.; Bawendi, M. G., Surface-Enhanced Emission from Single Semiconductor Nanocrystals. *Physical Review Letters* **2002,** *89* (11), 117401.

90. Jiao, Y.; Ryckman, J D.; Ciesielski, P. N.; Escobar, C. A.; Jennings, G. K.; Weiss, S. M., Patterned nanoporous gold as an effective SERS template. *Nanotechnology* **2011,** *22* (29), 295302.

91. Giersig, M.; Mulvaney, P., Preparation of ordered colloid monolayers by electrophoretic deposition. *Langmuir* **1993,** *9* (12), 3408-3413.

92. Teranishi, T.; Hosoe, M.; Tanaka, T.; Miyake, M., Size Control of Monodispersed Pt Nanoparticles and Their 2D Organization by Electrophoretic Deposition. *The Journal of Physical Chemistry B* **1999,** *103* (19), 3818-3827.

93. Van der Biest, O. O.; Vandeperre, L. J., ELECTROPHORETIC DEPOSITION OF MATERIALS. *Annual Review of Materials Science* **1999,** *29* (1), 327-352.

94. Zhitomirsky, I.; Gal-Or, L., Electrophoretic deposition of hydroxyapatite. *Journal of Materials Science: Materials in Medicine* **1997,** *8* (4), 213-219.

95. Islam, M. A.; Xia, Y.; Telesca, D. A.; Steigerwald, M. L.; Herman, I. P., Controlled Electrophoretic Deposition of Smooth and Robust Films of CdSe Nanocrystals. *Chemistry of Materials* **2003,** *16* (1), 49-54.

96. Hecht, S.; Hsia, Y. U. N., Dark Adaptation Following Light Adaptation to Red and White Lights. *J. Opt. Soc. Am.* **1945,** *35* (4), 261-265.

97. Gosnell, J. D. A Phosphor-based Light-emitting Diode Using White-light Cadmium Selenide Nanocrystals. Vanderbilt University, Nashville, TN, 2010.

98. Thornton, W. A., Spectral sensitivities of the normal human visual system, color-matching functions and their principles, and how and why the two sets should coincide. *Color Research & Application* **1999,** *24* (2), 139-156.